UPPSALA
UNIVERSITET

Digital Comprehensive Summaries of Uppsala Dissertations from the Faculty of Science and Technology 636

Studies of Unusual Seismicity and Long Period Events at the Glacier Overlain Katla Volcano, Iceland

KRISTÍN JÓNSDÓTTIR

ACTA
UNIVERSITATIS
UPSALIENSIS
UPPSALA
2009

ISSN 1651-6214
ISBN 978-91-554-7500-0
urn:nbn:se:uu:diva-100771

Dissertation presented at Uppsala University to be publicly examined in Hambergssalen, Geocentrum, Villavägen 16, Uppsala, Friday, May 8, 2009 at 10:00 for the degree of Doctor of Philosophy. The examination will be conducted in English.

Abstract

Jónsdóttir, K. 2009. Studies of Unusual Seismicity and Long Period Events at the Glacier Overlain Katla Volcano, Iceland. Acta Universitatis Upsaliensis. *Digital Comprehensive Summaries of Uppsala Dissertations from the Faculty of Science and Technology* 636. 85 pp. Uppsala. ISBN 978-91-554-7500-0 .

Earthquake catalogues are usually dominated by diffusive behaviour consistent with the Omori law of aftershocks. This is investigated in terms of waiting times, i.e. the time between successive events in a time-sorted earthquake catalogue. The theoretical waiting time probability distribution for the Omori law is derived and shown to predict the numerically produced Omori aftershock sequence well. These results enhance our understanding of aftershock processes and demonstrate that previous waiting time interpretations were severely flawed.

Iceland earthquake catalogues are studied in terms of waiting times. Omori aftershock sequences are shown to predict most datasets well but there are some significant exceptions. One of these is data from the glacier covered Katla volcano in South Iceland, with few aftershocks. This dataset can be further split into two geographical groups: Several hundred volcano-tectonic earthquakes occurring within the caldera, reaching depths down to 15 km, and thousands of emergent low frequency earthquakes with a poorly defined shallow source in Goðabunga, in the western part of Katla. These events are investigated further.

The lp events at Goðabunga have been recorded for decades and show a clear seasonal and climate-related correlation where their number increases in the autumn as well as during warmer years. Many of them form groups with very with similar waveforms. New broad-band seismic data suggests that the lp events originate in a steep outlet glacier covering Katla. Here, ice movement leads to ice falls over the steep escarpment, and we now believe that the lp events are generated by large ice falls rather than being related to gas or magma movements within the volcano, and are not precursors to an eruption as previously suspected. This observation probably has major significance for hazard estimation at the many ice-covered volcanoes around the world.

We report near-field (vlp) signals simultaneous with the largest lp events. Our data is partly consistent in character with surface deformation (displacement and tilt) due to the ice movements. However, in line with results from elsewhere, the magnitudes of the observed effects are large relative to those from mathematical modelling. Our analysis suggests that the signal is not an instrumental artefact. Possible explanations are discussed.

Keywords: waiting time distributions, lp-events, seasonal seismicity, vlp-signals, Katla volcano, Mýrdalsjökull, ice fall events

Kristín Jónsdóttir, Department of Earth Sciences, Geophysics, Uppsala University, SE-75236 Uppsala, Sweden

ISSN 1651-6214
ISBN 978-91-554-7500-0
urn:nbn:se:uu:diva-100771 (http://urn.kb.se/resolve?urn=urn:nbn:se:uu:diva-100771)

„Það bar til eitt sinn í Þykkvabæ er þar var munkasetur að ábóti hélt matselju er Katla hét. Hún var forn í skapi; hún átti þá brók að hvur sem í hana fór þreyttist eigi á hlaupum. Sauðamaður ábóta hét Barði; hann sætti þungum ákúrum af Kötlu þegar vantaði af fénu. Eitt haust fór Katla í veislu; þá fann sauðamaður ekki féð, tekur hann þá brók Kötlu og fer í og hleypur sem af tekur og finnur allt fáð, Þegar Katla kom heim verður hún vör við að drengurinn hefir brúkað brók hennar, tekur hann með leynd og kæfir í sýrukeri sem þar stóð í karldyrum að fornum sið. Þegar leið á vetur og ganga fór á sýruna, heyrðu menn Kötlu segja:"Senn bryddir á Barða." Þá gat hún ekki lengur leynst og tekur brók sína og hleypur út úr klaustrinu norðvestur til jökulsins og steypis sér þar í gjána að menn héldu, því aldrei sást hún síðan. Brá þá svo við að hlaup kom úr jöklinum og stefndi á klaustrið og Álftaverið, var það eignað fjölkynngi Kötlu og er gjáin síðan nefnd Kötlugjá."

\- Jónas Hallgrímsson

List of Papers

This thesis is based on the following papers, which are referred to in the text by their Roman numerals.

I Jónsdóttir K., M. Lindman, R. Roberts, B. Lund, R. Böðvarsson (2006), Modelling fundamental waiting time distributions for earthquake sequences, *Tectonophys.*, 425 (3-4):195–208.

II Lindman M., K. Jónsdóttir, R. Roberts, B. Lund, R. Böðvarsson (2005), Earthquakes descaled: On waiting time distributions and scaling laws. *Phys. Rev. Lett.*, 94, 108501.

III Jónsdóttir K., A. Tryggvason, R. Roberts, B. Lund, H. Soosalu, R. Böðvarsson (2007), Habits of a glacier covered volcano; Seismicity and structure study of the Katla volcano, South Iceland, *Ann. Glac.*, 45 :169-177.

IV Jónsdóttir K., R. Roberts, V. Pohjola, B. Lund, H. Shomali, A. Tryggvason, R. Böðvarsson (2009), Lp-events at Katla volcano, Iceland, are glacial and not volcanic in origin, *Submitted to GRL*

V Jónsdóttir K., B. Lund, R. Roberts, R. Böðvarsson (2009), Investigation of very long period seismic signals recorded at Mýrdalsjökull glacier, south Iceland, *Manuscript.*

Reprints were made with permission from the respective publishers.
Additional publications written during my stay at Uppsala University but not included in the thesis:

- Soosalu H**.,** K**.** Jónsdóttir, P. Einarsson (2006), Seismicity crisis at the Katla volcano, Iceland – signs of a cryptodome? *J. Volc. Geoth. Res.*, 153, 177-186.
- Lindman M., B. Lund, R. Roberts, K. Jónsdóttir (2006), Physics of the Omori law: Inferences from interevent time distributions and pore pressure diffusion modelling. *Tectonophys.*, 424 (3-4), 209-222.
- Lindman M., K. Jónsdóttir, R. Roberts, B. Lund, R. Böðvarsson (2006), Reply to comment on “Earthquakes descaled”. *Phys. Rev. Lett.*, 96, 109802.

Contents

Abbreviations

AZO	Azores islands
CGFZ	Charlie Gibbs Fracture Zone
EUR	European Plate
EVFZ	Eastern Volcanic Flank Zone
EVZ	Eastern Volcanic Zone
FK-analysis	Frequency–wave number analysis
H	Hengill
JMFZ	Jan Mayen Fracture Zone
KOL	Kolbeinsey island
LP	Long period
MAR	Mid Atlantic Ridge
Mc	Magnitude of completeness
NA	North American Plate
NVZ	Northern Volcanic Zone
RP	Reykjanes Peninsula
SIL	South Iceland Lowland seismic network, Iceland's regional network.
SISZ	South Iceland Seismic Zone
SP	Snæfellsnes Peninsula
SQRT	Square root
STF	Source time function
TFZ	Tjörnes Fracture Zone
V	Vatnajökull
VLP	Very long period
Vm	Vestmannaeyjar
WF	West Fjords
WVZ	Western Volcanic Zone

1 Introduction

Earthquake seismology has proven successful in extracting information about the interior of our Earth and about processes occurring inside the Earth, usually not visible to our eyes. Despite the fact that one should always be careful of relying only on one set of measurements, the constantly evolving seismological methods are many and they cover a wide range: From statistical approaches which deal with large datasets recorded on many stations, spanning tens of years and thousands of events, to detailed waveform analyses of a single trace. The different approaches and methods in seismology thus provide different information and boundary conditions in our attempt to unravel the mysteries of the Earth's structure and the physical processes that shape it.

One of the most interesting places to study our active Earth is in volcanic areas. Here the seismic activity rate can be high and the internal structure is usually very complex. In addition, the research is not only interesting for the scientific community but also for the public. In Iceland there is on average one volcanic eruption every fifth year. There are approximately forty active volcanoes, of which half have erupted in the last 1,000 years. Although most eruptions have been harmless shows of basaltic fissure opening, some volcanoes have erupted violently causing severe problems for the inhabitants of the country. Katla volcano in south Iceland is in this latter category.

At the southern end of the Icelandic Eastern Volcanic Zone (EVZ) we find four glacier-overlain volcanoes. Three of them have the same name as their respective glaciers, but the biggest one bears the name of Katla, an evil ogress. According to the sagas, she murdered a farm worker whom she suspected to have stolen her magic trousers. She hid the body at the bottom of a meat storage barrel filled with whey. As winter progressed there remained less and less in the barrel until one day the body of the farm worker Bardi was exposed. Katla ran away to the volcano and disappeared. Shortly after this happened, the volcano erupted. The story of Katla lives with the Icelanders and when an imminent eruption is feared they quote the words of Katla: “Senn bryddir á Barda” which translates to “Soon Bardi will be exposed”.

With two eruptions every century since the settlement of Iceland an eruption was expected already in the 1960's, but at the time of writing the vicious female troll has not yet erupted. Seismically, however, Katla, has been far from quiet. The seismic behaviour has also been atypical in many ways. Studies of the various parameters of the large earthquake dataset which has been collected by the Icelandic SIL network have clearly revealed the anomalous behaviour. The earthquakes do not occur randomly throughout the year. The bulk of the earthquakes are of exceptionally long duration and show mainly long period waves which are difficult to correlate with the typical earthquake phase arrivals. This and the fact that many arrivals are very emergent makes all routine analysis difficult, since it introduces errors e.g. in the earthquake locations.

The motivation for this PhD thesis is to investigate the extraordinary seismic behaviour and earthquake signatures which have been plaguing Katla for years. Where do they really occur? Why are the seismic signatures so long? And why do we always get more earthquakes in the autumn? This investigation is important for several reasons, not only scientific but also practical. In Iceland it is of great importance to be able to forecast eruptions and resulting catastrophic glacial floods.

My research has been focused on geothermal, volcanic and glaciated areas were the processes are often poorly understood and, to make problems worse, the Earth's structure can be complex. I strive to use various well established methods in earthquake seismology as well as to develop my own methodologies in order to maximise the amount of information I can extract from the data.

2 Tectonic setting of Iceland and the SIL seismic network

2.1 Brief introduction to the tectonics of Iceland

Iceland is a topographic anomaly situated on the Mid-Atlantic Ridge where the North American plate and the Euroasian plate drift apart at approximately 2 cm per year (*Sigmundsson*, 2006) (Figure 2.1). Iceland probably owes its very existence to a mantle plume (*Morgan*, 1971) which produces excessive amounts of magma and created the island about 15 million years ago (*Sigmundsson*, 2006).

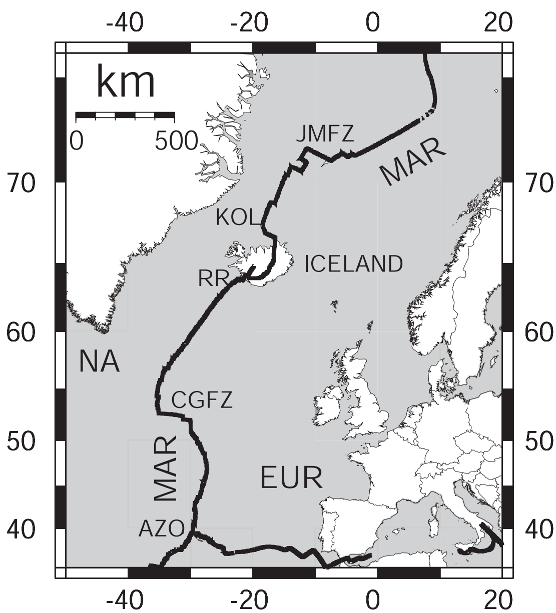

Figure 2.1 Iceland is situated on the slowly spreading Mid Atlantic Ridge (MAR) which comes onshore and splits the island between the North American Plate (NA) and the European Plate (EUR). The segment of the MAR which comes onshore at the southwestern tip is the Reykjanes Ridge and the segment north of the island is named after Kolbeinsey (KOL). The major fault zones on MAR, The Charlie Gibbs Fracture Zone (CGFZ) and the Jan Mayen Fracture Zone (JMFZ) as well as the triple junction at the Azores islands (AZO) are marked. Plate boundaries are collected from Coffin et al. (1998) and Jóhannesson and Sæmundsson (1998).

The plate spreading across Iceland is taken up within a 100-150 km wide plate boundary zone that coincides with volcanic zones (e.g. *Árnadóttir et al*., 2009). From the southwestern tip of Iceland, where the Reykjanes ridge comes onshore, plate spreading is accommodated by oblique rifting along the Reykjanes Peninsula (RP) extending to the triple junction at the Hengill volcano. There the rift branches into the Western Volcanic Zone (WVZ) and the South Iceland Seismic Zone (SISZ). The WVZ extends in a north-north-east direction to Langjökull glacier and according to GPS measurements the plate spreading rates increase north to south in the WVZ, from 2.6 to 7.0 mm/yr, respectively (*LaFemina* et al, 2005).

The SISZ is a left-lateral transform zone where the plate boundary deformation does not occur on a single east-west striking transform fault. Instead, relative plate motion is accommodated by an array of north-south striking right-lateral faults where moderate sized earthquakes (M6-7) rupture the brittle part of the crust. This mechanism has been given the term bookshelf tectonics (*Einarsson et al*., 2008, *Sigmundsson et al*., 2006). There is a change in direction of the plate boundary from the RP to the SISZ across Hengill, with significantly more opening across the RP than the SISZ. The WVZ extends north from Hengill, making it a triple junction. Although the SISZ is only defined as the region between the Torfajökull glacier in the east and the Hengill triple junction in the west, the array of north-south striking faults continues to the west through the Reykjanes Peninsula (*Einarsson,* 2008). When large historic earthquakes are investigated in south Iceland (*Sigmundsson*, 2006), it becomes clear that the transform zone extends in fact from Torfajökull glacier in the east, westwards through the Reykjanes peninsula, covering an area of 150 x 10 km (see Figure 2.2).

At the western end of the SISZ, almost parallel to the WVZ, lies the Eastern Volcanic Zone (EVZ) where the rift continues northwards. From north, the zone extends from the Bárðarbunga and Grímsvötn central volcanoes within the Vatnajökull glacier, considered to be the center of the hotspot, and is usually considered to end at the intersection with the SISZ where the Eastern Volcanic Flank Zone (EVFZ) continues south-westwards. North of Vatnajökull the continuation of the EVZ is termed the Northern Volcanic Zone (NVZ). Here the volcanic zone bends and continues to the north, via e.g. the Krafla fissures and ends were it meets the Tjörnes Fracture Zone (TFZ). It is a right lateral transform zone, extending 150 km in an east-northeast direction from the NVZ to the submarine Kolbeinsey Ridge, north of Iceland. The complex fracture zone consists of three parallel lineaments, the Grímsey Lineament, the Húsavík-Flatey Fault and the Dalvík Lineament, each with its own style of structure and patterns of seismicity (*Sigmundsson* 2006).

The spreading rates are higher in the EVZ than in the WVZ, decreasing north to south from 19.8 to 8 mm/yr (measured just north of Mýrdalsjökull). From the southern end of the EVZ the EVFZ extends to the Vestmannaeyjar islands (*LaFemina et al*. 2005). *Sigmundsson* (2006) refers to same flank zone as the South Iceland Flank Zone. The EVFZ is considered to be outside the active plate boundary and thus the name flank zone.

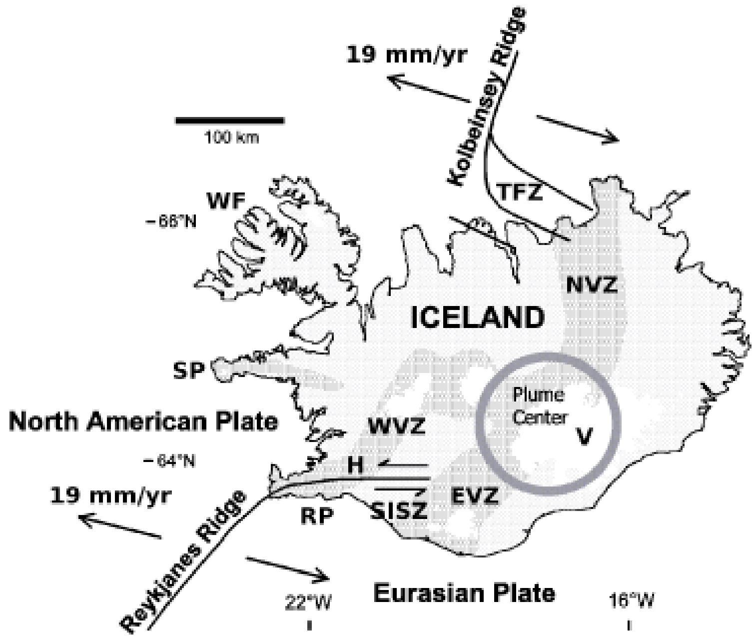

Figure 2.2. The Tectonics of Iceland. The Reykjanes Ridge, a section of the Mid-Atlantic Ridge (MAR) comes onshore at the south western corner of Iceland, the Reykjanes Peninsula (RP). The Hengill volcanic system (H) marks the junction between the RP, theWestern Volcanic Zone (WVZ) and the South Iceland Seismic Zone (SISZ), a transform fault zone which extends to the Eastern Volcanic Zone (EVZ). The plume center is currently believed to be situated beneath the northwest-ern part of Vatnajökull glacier. The Northern Volcanic Zone (NVZ), extends from north of Vatnajökull to the Tjörnes Fracture Zone (TFZ), a transform zone which accommodates plate motion between the NVZ and the northern continuation of the MAR, the Kolbeinsey Ridge. The rifting rate is approximately 19 mm/yr between the North American plate and the Eurasian plate. The current interpretation of the tectonics is that there exists a microplate, the Hreppar block, between the WVZ and the EVZ, just north of the SISZ. The Snæfellsnes Peninsula (SP) is a volcanic zone of low geothermal activity, as are parts of the West Fjords (WF). Original figure from Páll Einarsson, University of Iceland.

There are some structural differences between the EVZ and the EVFZ since significant crustal spreading has only developed in the EVZ, which is marked by fissure swarms and hyaloclastite ridges. Little spreading has occurred in the EVFZ where the structure is dominated by large central volcanoes. In addition the petrology changes from olivine thoelites in the north to transitional and alkali olivine basalts in the EVFZ (see Figure 2.3).

The WVZ has been active since 7-9 Ma, when the plate spreading jumped from the Snæfellsnes Peninsula to the east. Similarly the EVZ formed at 2-3 Ma during the last eastward migration of spreading (*Sæmundsson*, 1974). The EVZ is belived to be a propagating rift zone moving to the south-west at speeds of 35-50mm/yr (*Einarsson*, 1991).

Due to the overlapping rift segments in south Iceland a micro plate, the Hreppar block, has been postulated north of the SISZ, from the WVZ to the EVZ (*Einarsson* 1991, *Sigmundsson* et al., 1995). Recent GPS data from the Hreppar block fit a rigid block model within uncertainties (*LaFemina et al*., 2005).

Seismic constraints reveal a crustal thickness in Iceland from 8 to 40 km. The thickest crust is found above the centre of the mantle plume (*Darbyshire et al*. 1998, *Allen et al*., 2002a, 2002b).

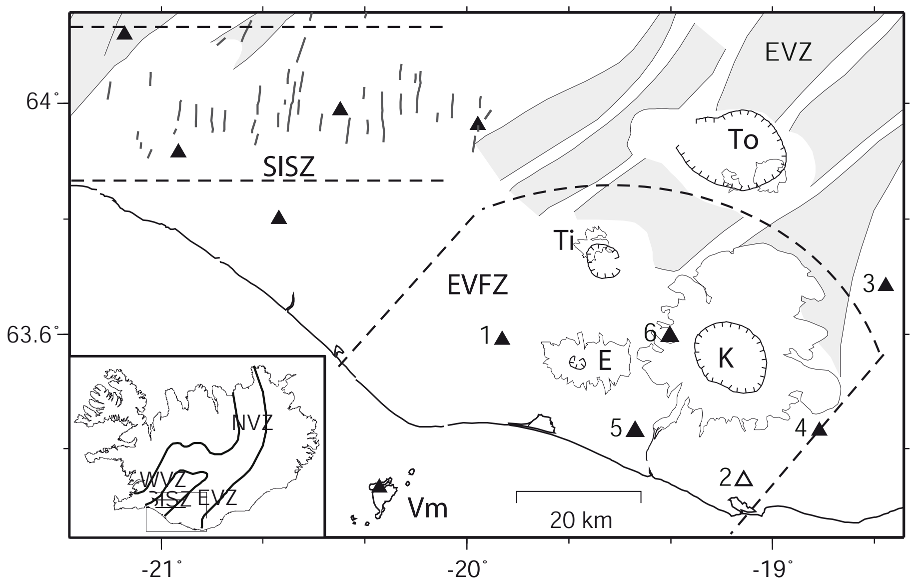

Figure 2.3. The tectonic setting of the Katla volcano which resides in the Eastern volcanic flank zone (EVFZ) together with Eyjafjallajökull volcano (E),Tindfjallajökull volcano (Ti) and the Vestmannaeyjar volcanic islands (Vm). Just north of Katla, in the Eastern volcanic zone (EVZ) is the Torfajökull volcanic region (To). The south Iceland seismic zone (SISZ) is marked. The inset in the lower left corner illustrates which part of Iceland we are looking at. Black triangles show the stations of the SIL system. Numbers refer to time of installation (discussion in 2.7.1). Station 1, MID, station 2 SKH, was moved to station 5 ESK in 2001, station 3 SNB, station 4 HVO and station 6 GOD.

2.2 The geological settings of Katla volcano

The volcanic zones in Iceland encompass a number of central volcanoes, i.e. a volcanic edifice which is usually associated with silicic rocks and high temperature geothermal areas. These central volcanoes are as a rule transected by extensive fissures and normal faults and together they make up a volcanic system (*Einarsson*, 1991).

In the EVFZ, surrounded by three smaller volcanoes bearing the names of their overlaying glaciers, we find Katla, one of the most active volcanic systems in Iceland. The Katla volcanic system consists of a hyaloclastite massif which reaches 1380 m. a. s .l. and is structurally connected to the 60 km long Eldgjá fissure, which extends from the north-eastern part of the central volcano towards the Eastern Volcanic Zone (*Larsen*, 2000). The massif encompasses a huge oval caldera (9 x 14 km in diameter) elongated in the direction of the rift zone. The elongation of the caldera is probably a fault distortion effect in the active tectonic setting of the rift zone (*Holohan et al*. 2005) and not the effect of post formation deformation caused by the rift spreading as proposed in Paper III. The caldera formation model of *Holohan et al*. (2005) better explains the discrepancy between the ages of the caldera and the ellipticity and implies that if the system was tectonically active at the time of caldera formation then the ellipticity is of limited use in reconstructing the spreading.

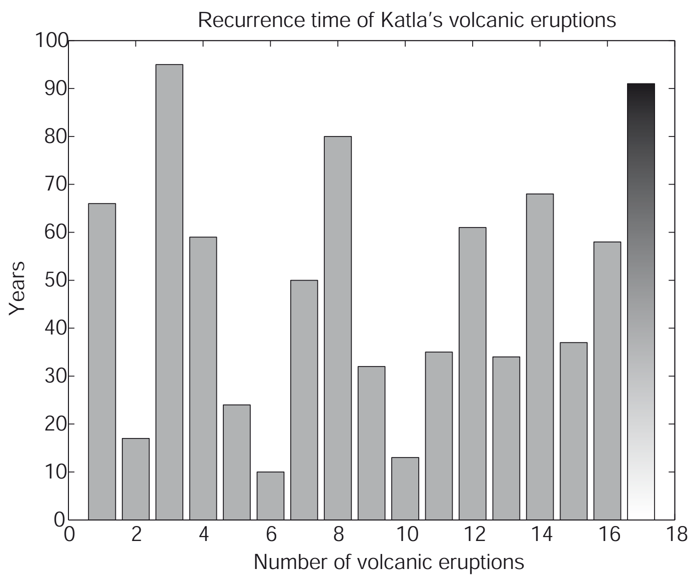

Figure 2.4. The histogram represents the time between Katla's eruptions i.e. the recurrence time in years of volcanic eruptions since year 1179, with the horizontal axis being essential a time axis from 1179. The figure clearly shows that we are now (column farthest to right) experiencing an unusual long period of quiescence, or the longest period of quiescence since between 1262 and 1357.

Katla is overlain by the fourth largest glacier on the island, Mýrdalsjökull. The ice-filled 600m deep caldera (*Björnsson et al*., 2000) forms a glacier plateau at an elevation of around 1300m, surrounded by higher rims. The glacier surface is marked with about a dozen circular depressions 0.5-1 km wide and 20-50 m deep known as cauldrons. These are created by geothermal activity and involve water concentrations beneath the ice sheet (*Björnsson et al.* 2000).

Katla eruptions are usually accompanied by tephra fall, lightning and hazardous jökulhlaups. The volcano erupted quite regularly about twice per century in historic times but there has been no visual eruption since 1918. This is the longest recorded period of quiescence since between years 1262-1357, see Figure 2.4, which could imply that an eruption is now overdue. Volcanism within the Katla volcanic system during the Holocene has been characterized by: 1) explosive (phreatomagmatic) basaltic eruptions along volcanic fissures within the Mýrdalsjökull caldera (most common); 2) explosive silicic eruptions from vents associated with the caldera and 3) predominantly effusive basaltic eruptions involving both the central volcano and the fissure swarm (*Larsen*, 2000).

In a review paper on seismic structure in Iceland, by *Brandsdóttir and Menke* (2008), they estimate from the different studies that the Moho depth beneath Katla is 25 km.

A summary of former studies of earthquake activity as well as the plumbing system of Katla is given in Paper III and in (2.6) which discusses recent deformation studies of Katla.

2.3 Recent activity of Katla and Eyjafjallajökull volcanoes

The last Katla eruption occurred in 1918 and was accompanied by massive jökulhlaups flooding the plains south of the glacier. Amazingly the flood did not cause any casualties but lightning in the volcanic plume caused two fatalities. In June 1955 and in July 1999 small jökulhlaups occurred in the river which drains the outlet glacier Sólheimajökull (southern Mýrdalsjökull).

Katla and Eyjafjallajökull volcanoes are situated 25 km apart and have a history of simultaneous volcanic activity. The much more active Katla volcano has erupted at least 20 times in historic times while Eyjafjallajökull's two eruptions were contemporaneous with Katla eruptions. Seismic swarms recorded beneath Eyjafjallajökull increased in 1994 and again in 1999. The activity culminated in July 1999 when a shortlived but powerful pulse in geothermal heat output took place followed by a flash flood from Sólheimajökull. The event was associated with seismicity, bursts of tremor, and the formation of three new ice cauldrons.

After the events in 1999, a decline in geothermal activity was observed. In 2001-03 some ice cauldrons expanded and deepened by 10-15 m, indicating renewed increase in geothermal activity. This trend is also apparent for 2003-05. The increase in geothermal power amounts to a few tens of megawatts. It is likely that the increased thermal output is related to increased volcano tectonic seismicity and is caused by magma inflow (*Vogfjörð et al.*, 2008).

The 1999 increase in seismicity at Eyjafjallajökull was associated with significant inflation of the volcano. Deformation data was modeled with a point pressure source at 3.5 km depth beneath the flank of the volcano, about 4 km south of the summit crater. Maximum uplift of the model is 0.35 m (*Pedersen & Sigmundsson*, 2006). A similar model also explains deformation associated with the 1994 seismic crisis (*Pedersen & Sigmundsson*, 2004). The deformation field of the Katla volcano is more difficult to ascertain due to the extensive glacier coverage.

Another episode of increased seismicity started in 2001 west of the Katla caldera. There has been no visual eruption, and neither jökulhlaups nor significant changes in the ice cauldron depths (which are measured twice a year) have been observed. Seismicity in the western part of the glacier overlain volcano started to increase, slowly but gradually and still showed strong annual variations, leading to discussions of a possible imminent Katla eruption.

2.4 Katla volcano monitoring

Following the jökulhlaup in July 1999, a comprehensive monitoring program was set up for Katla, including ice surface elevation profiling from aircraft carried out twice a year by the University of Iceland to monitor variations in geothermal heat and detect signs of subglacial water accumulation, using an automated system based on ground-clearance radar and kinematic GPS (*Guðmundsson et al.*, 2007). A radar altimeter coupled with a kinematic GPS gives an absolute elevation accuracy of 3 m and internal consistency of 1-2 m. An annual accumulation-ablation cycle in surface elevation with amplitude of 5-10 m is observed. By removing this cycle from the data, changes due to subglacial geothermal activity are obtained (*Guðmundsson et al.*, 2007).

In addition inspection flights on a small plane are carried out about once a month from the village of Vík, south of Mýrdalsjökull. The volcano is currently monitored with one web camera which has been installed south of Katla (http:/www.ruv.is/katla). The project is run cooperatively by the Police, the Iceland Telecom and the Icelandic National Radio.

The Icelandic Meteorological Office runs a seismic network (SIL, see discussion in 2.7) which currently includes four stations around the volcano (of which one has a broadband sensor) as well as two GPS stations that record continuously.

Measurements of soluble chemicals are manually and automatically conducted in some glacial rivers that drain Mýrdalsjökull glacier. An increase of those can be a sign of volcanic unrest. In addition, river height and flow is monitored.

Manual tilt measurements have been conducted irregularly (sometimes a few measurements per year, and some years no measurements) since 1967 by the Nordic Volcanological Center in Iceland. Since the data is sparse it was not included in this study.

2.5 Mýrdalsjökull ice cap

Mýrdalsjökull is the forth largest temperate glacier on the island. It is located where precipitation is measured to be around the highest in Iceland, above 2000 mm/yr (data from the Icelandic Meteorlogical Office). Studies of Mýrdalsjökull are many but unfortunately some measurements have not been regular and thus a good record of the glacier changes over a time period of several years does not exist. I will briefly summarize the latest findings regarding the glacier.

Guðmundsson et al. (2007) study ice cauldrons and ice cauldron changes using techniques that have already been described (see 2.4). They report 16 cauldrons located above the rim of or inside the caldera.

Scharrer et al. (2008) analysed a total of 30 synthetic aperture radar (SAR) images with special focus on identifying circular and linear depressions in the glacier surface with a constant location. Such features are indicative of sub-glacial geothermal heat sources and formations of sub glacial lakes and the adjacent sub-glacial tunnel (melt water drainage) system. The time series comprises images from five different SAR sessions covering a time period of 12 years, starting in 1994. Twenty permanent ice cauldrons (150-250 m in diameter) could be identified within the caldera and four semi-permanent on (or marginally outside) the eastern caldera rim. Some of these had not been identified before by *Gudmundsson et al*. (2007). All cauldrons are connected to tunnel systems for melt water drainage. More than 100 km of the sub-glacial drainage system could be identified beneath the Mýrdalsjökull ice cap, each tunnel originating at an ice cauldron (geothermal area) or connecting the geothermal areas. *Scharrer et al.* (2008) present a new piecemeal caldera model of the caldera based on the spatial distribution of the geothermally active areas. Instead of the elliptical caldera based on the topographic rim which *Björnsson et al.* (2002) suggest (see Figure 2.3), *Scharrer et al*. (2008) present a near circular caldera coinciding with the topographic caldera rim in the northern part and a half circular section caldera in the southern part.

Scharrer et al. (2008) conclude that the subglacial lakes are drained through the outlet glaciers Entujökull (north west) and Sléttjökull (north) furthermore they conclude that the tunnel systems are not in total agreement with estimated water divides from *Björnsson et al.* (2000). It is however important to note that all of the above mentioned studies do agree on that there is no sign of a geothermal source existing beneath Tungnakvislarjökull outlet glacier or the other western outlet glaciers. In addition none of the sub-glacial water concentrations are drained via the western outlet glacier except via Entujökull in the north west.

Recent analysis of sulphur concentrations in tephra layers suggests that over the last at least 8400 years, explosive activity at Katla has been dominated by phreatomagmatic eruptions, implying that the Mýrdalsjökull ice cap has been present throughout the Holocene (*Óladóttir et al.* 2007).

2.5.1 Tungnakvíslarjökull outlet glacier

The beautiful Tungnakvíslarjökull is the biggest of the western outlet glaciers and falls off steeply just north of the ridge Fimmvörðuháls between Mýrdalsjökull and Eyjafjallajökull glaciers. The hike between the glaciers is one of the most popular trails in Iceland during the summer months and in clear weather the Tungnakvíslarjökull glacier is one of the most spectacular sights on the way. The glacier dips steeply towards the west in an icefall and encompasses at least one great escarpment from which ice blocks will inevitably fall (see Figure 2.5). It is important to note that the dramatic ice fall is at least 5 km away from the trail and therefore it is difficult to observe an ice fall event without special equipment. Tungnakvíslarjökull is surrounded by steep hills and hyaloclastite ridges. The sound of rumbling has been heard by many people but the visual observation of such an ice fall event has not been confirmed.

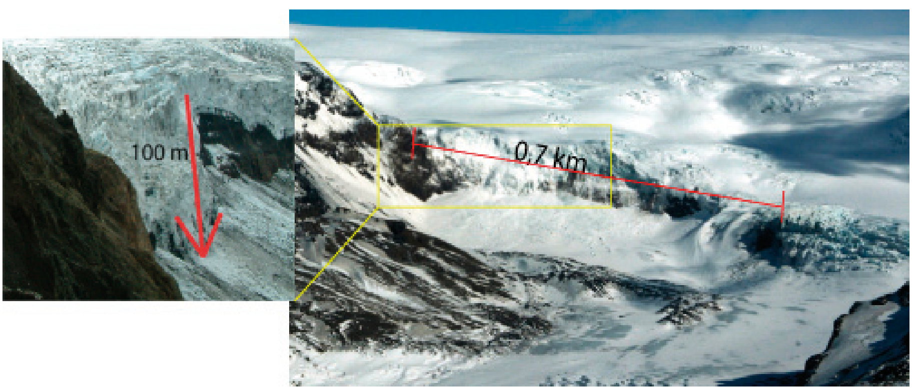

Figure 2.5. Photos of the upper part of Tungnakvíslarjökull outlet glacier. Photo on the left was taken in April and the photo on right was taken during the summer. The ice fall is clearly seen as well as rockslides that cover part of the glacier. (Photos: Jósef Hólmjárn)

From photos it is obvious that these hills, especially the very steep slope north of Tungnakvíslarjökull, are not all that stable and rock falls do occur resulting in screes that cover lower parts of the outlet glacier.

Björnsson et al. (2000) measured ice thickness of large parts of Mýrdalsjökull but for obvious reasons the heavily crevassed upper part of Tungnakvíslarjökull was poorly recorded. Above Tungnakvíslarjökull values of around 150-200 m are estimated which increase dramatically towards the caldera where ice thickness is measured to be around 600 m.

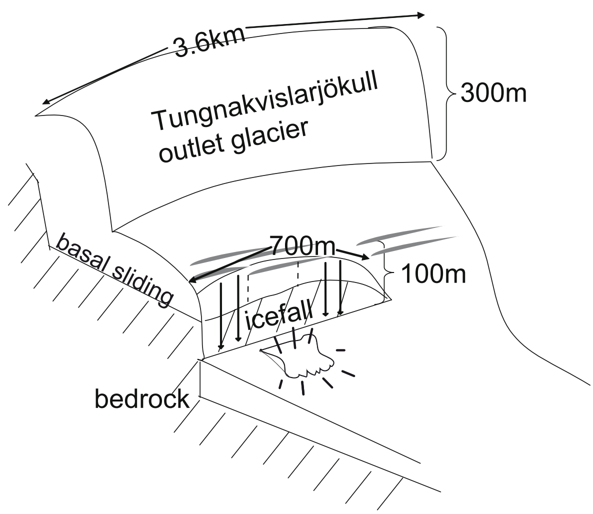

Figure 2.6. A simplified sketch of Tungnakvíslarjökull outlet glacier which falls steeply into a valley west of Mýrdalsjökull. The glacier is viewed from north. The sketch is based on photographs (from Jósef Hómjárn in 2000 and 2002) as well as maps (Landmælingar Íslands).

2.6 Katla and deformation

There is an ongoing debate among scientists as to whether or not there was a magmatic intrusion episode at Katla volcano, between 1999 and 2004, causing an uplift of the area as well as raising the level of seismicity.

Pinel et al., (2007) model surface displacements induced by ice load variation through time by spatial integration of Green's function for an elastic half-space, which allows for displacements caused by short-term (seasonal) variations, and a thick elastic plate lying over a viscous mantle, describing the final relaxed state. Seasonal vertical displacements measured from 2000 to 2006 at two continuous GPS stations located near the edge of Mýrdalsjökull ice cap fit well to their model of an elastic response to the annual variation in ice load. But a forward model considering an elastic thickness of 5 km can only explain a fraction of the uplift recorded from 1999 to 2004, and it cannot account for the observed horizontal velocities. They conclude that magma inflow is required to explain observed inflation of the Katla volcano 1999–2004.

Sturkell et al. (2008) used geodetic observations on nunataks and in the vicinity of Mýrdalsjökull, together with seismic and ice-surface observations, to infer a magma intrusion in the north-eastern part of the caldera between 1999 and 2004. The GPS observations are modelled with a point source at 4.9 km depth. The authors discuss the possibility that the observed vertical velocities could be explained by glacial isostatic adjustment due to the melting glacier alone, but conclude that the observed horizontal velocities cannot. They adjust their inflation source to 2-3 km depth to account for the glacial isostatic adjustment process. *Sturkell et al.* (2008) also conclude that the seismic source at Goðabunga does not produce a detectable signal at their geodetic stations and that the source therefore must be shallow. They point out that a hypothesized migrating cryptodome in the area could be reconciled with the data.

Árnadóttir et al. (2009) analysed GPS data from two country wide campaigns in 1993 and 2004, together with all the available continuous GPS data. They show that the vertical velocities in Iceland are dominated by the glacial isostatic adjustment process and that local GPS analyses must take large scale glacial isostatic adjustment into account. For Mýrdalsjökull, *Árnadóttir et al.* (2009) find that the observed vertical velocities are slightly smaller than those predicted by the preferred glacial isostatic adjustment model (in contrast to *Pinel et al.'s* , 2007, model), but that the horizontal velocities are significantly higher (in agreement with *Pinel et al.'s* , 2007, model). They suggest that this may be due to rheological structure and fast deglaciation rates that have not been accounted for in the model and argue that significant magma accumulation at shallow depth is not indicated by the data during 1993 - 2004.

Based on data from a temporary network of four seismometers installed on nunataks in 2003, *Soosalu et al.* (2006) find that the earthquakes at Goðabunga are shallow, within the uppermost 2 km, concentrated in a small area with a diameter of 3 to 4 km. They speculate that the low frequency earthquakes at Goðabunga might be caused by an intruding cryptodome.

Vogfjörð et al., (2008) study earthquake activity within the caldera. Out of 3000 events recorded with the SIL network from 1991 to 2008, they study 1500 with good signal to noise ratio. The events are relocated in a new velocity model. *Vogfjörð et al.* (2008) speculate that a small influx of magma occurred in 1998 when events are located down to 20 km depth in a confined area in the north-eastern part of the caldera. They find a dramatic increase in seismicity extending into the lower crust between years 2002 and 2004. The hypocenters are found to be confined beneath the north-eastern caldera rim and in a north-south striking line through the center of the caldera. The western part of the caldera is found to be nearly aseismic.

Using persistent scatterer and combined multiple acquisition InSAR techniques, *Hooper and Pedersen* (2007) studied line-of-sight displacements for the area surrounding Katla between 1995 and 2003 (ERS data) and September 2003 to July 2006 (ENVISAT data). They find that the data is consistent with glacial isostatic adjustment, and that an intrusion of magma or fluids is not required to explain the data. *Hooper and Pedersen* (2007) conclude that the increased seismicity in the Goðabunga region was not accompanied by significant deformation.

2.7 The SIL network

The South Iceland Lowland (SIL) seismic network started as a collaborative project between the Nordic countries on earthquake prediction research in 1988. The project included the installation of seismic stations in the South Iceland Seismic Zone (SISZ) and the design of an earthquake data acquisition and analysis system (Stefánsson et al., 1993). Today the network has grown to monitor not only the active transform zones but also the rift zones. The SIL network currently consists of 56 stations, concentrated mainly in the SISZ and around Eyjafjallajökull and Mýrdalsjökull, north of Vatnajökull in the vicinity of the gigantic reservoir Hálslón and in the Tjörnes fracture zone, see Figure 2.7.

The highly automatic SIL system, which has been in operation since 1990, was designed to enable accurate locations, source parameter determination and fault plane solutions for earthquakes. In particular the design was focused on very small earthquakes (micro earthquakes) since they can provide a detailed view of the distribution of stresses within the crust, an essential factor for understanding earthquake processes and for earthquake prediction.

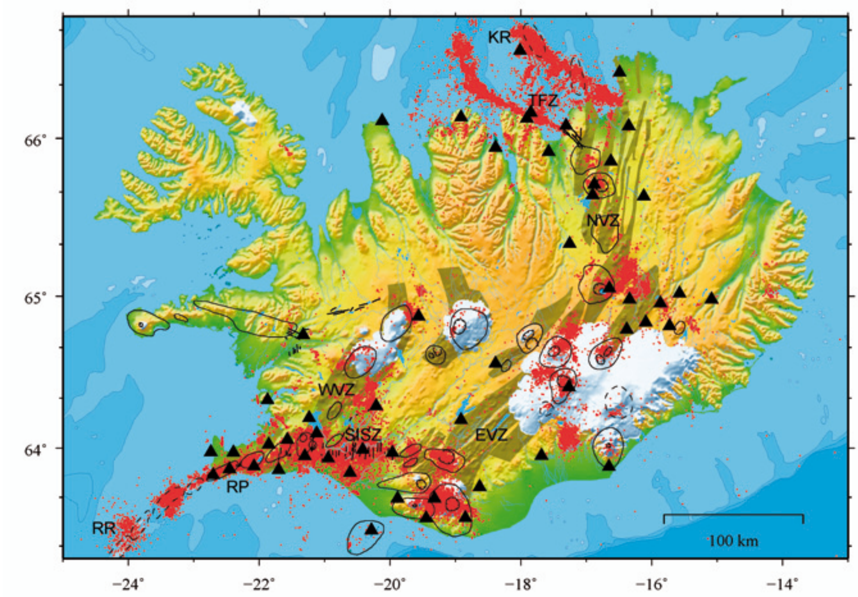

Figure 2.7. Map showing the SIL network (year 2008) which consists of 56 seismic stations marked with black triangles. Red dots denote earthquakes measured by the network between 2000 and 2007. The Reykjanes peninsula (RP), The Western Volcanic Zone (WVZ), the Eastern Volcanic Zone (EVZ), the South Iceland Seismic Zone (SISZ), the Northern Volcanic Zone (NVZ), the Tjörnes Fracture Zone (TFZ) and the Kolbeinsey Ridge (KR) are marked. (Original figure from Þóra Árnadóttir)

The description of the SIL network below is based on *Böðvarsson et al.* (1996). Each station is equipped with a three-component short period sensor (with the exception of a few broadband sensors) which is mounted on bedrock, a digitizer, a GPS synchronized clock and a PC running the Unix/Linux operating system. The SIL system uses single-station phase detections which are analysed to estimate onset time, duration, phase type (P or S), maximum amplitude, signal and noise averages, spectral parameters such as DC-level and corner frequency etc. Detected phases are periodically reported to a central computer with automatic algorithms to associate and locate events. Phases from the stations are associated using iterative location, phase truncation, amplitude consistency and negative evidence (stations without detections) to identify events. Waveform data is transferred to the central computer and analysed. The routine analysis performed on every recorded earthquake includes estimation of the focal mechanism. The system is designed around the most common earthquakes which have double couple fault plane solutions. Using grid search over source parameters radiation patterns are calculated. This systematic search not only finds the an "optimal" fault plane solution, but also generally provides a range of possible solutions which fit the data within a given limit.

In the SISZ, where the network is dense, the SIL catalogue is considered complete down to magnitude 0 (*Wyss & Stefánsson*, 2006). In the Katla volcanic area the magnitude of completeness has been 1.5 since 2001.

2.7.1 Station history around Mýrdalsjökull

In 1989 the SIL network started recording earthquakes in the area by installing MID, a station west of Eyjafjallajökull (see Figure 2.3). In 1992 the next station was installed south of Mýrdalsjökull (SKH). That station was moved in 2001 to ESK, a quieter place a little further the west, improving the observing capabilities significantly. In 1993 the third station, SNB, was installed in the area, east of Mýrdalsjökull. In 1999 a station HVO was installed south-east of Mýrdalsjökull. The station is installed on a low hyaloclastite ridge surrounded by glacial rivers. Due to high noise level at the site (probably from wind and the rivers) the station deployment did not change the detection capabilities significantly. The most recent station, GOD, was installed in September 2006 on a hyaloclastite ridge just north of Tungnakvíslarjökull outlet glacier. In the autumn of 2007 the short period sensor (Lennartz 3D-5sec) was replace by a broad band sensor (Guralp CMG-ESPC). Detection improvement has not been investigated with the addition of GOD.

2.7.2 The SIL /Goðabunga catalogue

Since the SIL system is designed for detecting "normal" earthquakes, unusual seismicity, such as that of Goðabunga, may be treated sub-optimally. For instance, the standard SIL waveform data extraction mechanism does not anticipate the long duration of the lp events, causing the latter part of the wave-train to be discarded. This is because the SIL system in its standard configuration only saves waveform data of presumed P and S waves of short duration after a normal, impulsive, event. These generally have shorter coda than the lp-events observed at Goðabunga. In addition, if the event is only observed at a few stations close to the event then the system automatically assumes the event is small and doesn't allow for low corner frequencies.

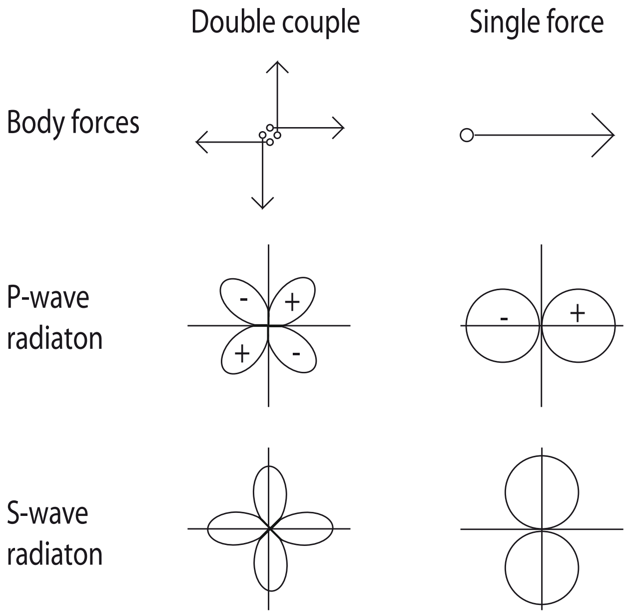

Figure 2.8. Schematic figures of the differences between a double couple and a single force source mechanism. The double couple mechanism is equivalent to slip on a fault (*Maruyama*, 1963). A single force model has been shown to agree well with e.g. landslides (*Kanamori et al.*, 1984)

Since the Goðabunga events are (most likely) not generated by a double couple source mechanism we get additional problems, since the SIL events are routinely analysed under the assumption of a double couple source. For non-double couple sources the estimated fault plane solutions will be at best inaccurate and at worst directly misleading. The model fit in the inversion for a double couple solution may give us a clear indication that the model is inappropriate, but neither this nor the estimated source parameters can necessarily indicate what the actual mechanism is.

Magnitude (seismic moment) calculations are also based on the double couple source model. The radiation pattern will be different for any other mechanism. Therefore energy for non-double couple events can be expected to be incorrectly estimated, and in fact there is not really a comprehensive definition of what "magnitude" means for these events.

The radiation patterns shown in figure 2.8 correspond to amplitudes which would be observed at distance if the Earth was a homogeneous whole-space. In reality, we have scaling effects due to the free surface and focussing effects, multi-pathing and phase conversion effects due to a non-homogeneous earth. It is thus clear that total energy based on the DC level of

P-waves from single force earthquakes are likely to be incorrectly estimated and we believe this to be the case for the Goðabunga events. There may also be a further bias because of the measurement configuration, especially for a single force, or a linear superposition of such forces, with the (main) force vector pointing west, because it is to the west that most of the SISZ sensors are located. Very few sensors are located south and north of Tungnakvíslarjökull i.e. where the minima of the single force P-wave radiation pattern is expected to be.

Despite inadequacies in the SIL system for dealing with unusual seismicity, it performs very well when it comes to detection. The system detects the events relatively robustly but the exact onset times and thus locations from the standard SIL system are not very reliable. The data collected with the temporary network GOD2007 (see section 4 in the thesis) verifies that the detection capability of the SIL system (at least in the area of Katla) is very good, and thus that information about the temporal pattern of Katla seismicity from the SIL system was reliable, even though the further measurements presented in this thesis significantly improve estimates of location, energy release and source characteristics.

3 Seismicity patterns

In attempts to unravel the mysteries that control where and when and why earthquakes happen scientists use different methodologies depending on what questions they are currently addressing. When it comes to questions regarding ongoing underlying physical processes it can be of great advantage to work with large data sets and extract information that gives us an averaged and a robust picture of what is going on. Here the recipe for success is a good and reliable dataset that is analysed using tools from statistics.

3.1 Temporal patterns

When a long time sequence of earthquakes is examined, we usually observe repeated patterns of activity. For example when the number of events are plotted as a function of time the general pattern of aftershock sequences is observed, where a great number of events occur close in time (as aftershocks to a large earthquake) followed by a rapid decay. As early as 1894, F. Omori presented an empirical relationship describing the rate of aftershock decay which is still today one of the best established relationships in statistical seismology (*Omori*, 1894).

Foreshocks preceding big earthquakes are sometimes recognized. An inverse Omori law has sometimes been used to describe their occurrence in time (e.g. *Peng et al.*, 2007) but statistical theories on foreshocks are not as well established as the data is currently too scarce.

Other temporal patterns are often very obvious in the earthquake data, and can be related to outside controlling factors, such as lowered detection due to urban activity during the daytime or other predictable periodic activity with a known or unknown underlying source. It is essential to try to reveal these sources in order to understand the earthquake record.

3.1.1 The Omori law

The modified Omori law of aftershock describes how the number of aftershocks decays with time after a large earthquake(*Omori,* 1894; *Utsu*, 1961; *Utsu et al*., 1995).

$$\frac{dn}{dt} = \frac{K}{(C+t)^p} \equiv \lambda(t) \tag{3.1}$$

Here n is the number of events following the main shock, K, C and p are empirical parameters and t is the time since the main shock. The parameter K is related to aftershock productivity (related to the size of the main shock and the seismic network capabilities). The parameter C describes aftershock rate at times very close to the mainshock and is currently debated. Some authors argue that C is zero but that the inability of seismic networks to measure earthquake activity close to a mainshock produces a non-zero C (e.g. *Kagan*, 2004). Others claim that physical processes acting immediately after a mainshock makes C non-zero and the aftershock rate roughly constant (e.g. *Lindman et al*., 2006). The parameter p describes the power law decay for t >> C.

3.1.2 Waiting time distributions

The term waiting time, delay time or inter-event time describes the time between successive events in a time-sorted catalogue. Analyses of waiting times have been done not only in seismic records but also in other fields. Waiting times are studied in Papers I and II, specifically following a homogeneous Poisson process and the non-homogeneous process where the rate of aftershocks following the Omori law has been investigated.

A common and convenient presentation of waiting times is to present them as histograms, i.e. to count the number of waiting times within a given range using bins of logarithmically increasing size. The y-axis representing the count of waiting times is often logarithmical too and sometimes scaled. A common scaling is to normalize with the width of each logarithmic waiting time bin. This gives us a scaled version of the probability density function (a proper probability density function has an area equal to one).

3.1.2.1 The homogeneous Poisson waiting time distribution

Events triggered at times described by the homogeneous Poisson process occur with a constant underlying rate irrespective of time or previous events. In other words, the events are statistically independent of each other and the expectation of the occurrence time is defined by the constant rate, μ, alone. This purely random behaviour is often taken as the null hypothesis for the occurrence of main shocks.

We map a time limited data series (total length T) into waiting time bins ranging from [Δt_1, Δt_2,…, Δt_i, Δt_{i+1},…, Δt_N] where Δt_N is the longest possible waiting time (less than or equal to the total length of our data). The Poisson probability density function, f(Δt), for waiting times is given by

$$f(\Delta t) = \mu e^{-\mu \Delta t} \tag{3.2}$$

By integrating the above probability density function (normalized) over the waiting time of interest, [Δt_i, Δt_{i+1}], and multiplying with the total number of waiting times, N_{tot}, (equals the total number of events-1) we get the count of waiting times that fall within the bin of interest.

$$\begin{aligned} N_{\Delta t_i - \Delta t_{i+1}} &= N_{tot} \int_{\Delta t_i}^{\Delta t_{i+1}} \mu e^{-\mu \Delta t} d(\Delta t) \\ &= N_{tot} e^{-\mu \Delta t_i} (1 - e^{-\mu (\Delta t_{i+1} - \Delta t_i)}) \end{aligned} \tag{3.3}$$

This equation describes the theoretical expectation for the count in each bin in the waiting time histogram and can be used to compare to real data.

3.1.2.2 The Omori waiting time distribution

Waiting time in an Omori aftershock distribution can be defined as the time from the main event, or as the time from the preceding aftershock. We use the latter definition. Equations describing the waiting time distributions following the Omori law of aftershocks are derived and discussed in Papers I and II. Despite the widely used Omori law, a description of its waiting time probability distribution as well as density function was not readily accessible before.

The equation, a general theoretical expression for the count of waiting times, $N_{T(\Delta ti - \Delta ti+1)}$, in the bin [$\Delta t_i$, Δt_{i+1}], is derived using the well known Poission probability distribution by studying the non homogeneous case with the rate following Omori's law (see equation 3.1).

$$N_{T(\Delta t_i - \Delta t_{i+1})} = \int_0^T \frac{K}{(C+t)^p} \left(e^{-\frac{K \Delta t_i}{(C+t)^p}} - e^{-\frac{K \Delta t_{i+1}}{(C+t)^p}} \right) dt \tag{3.4}$$

A theoretical expression for the Omori law waiting time probability density function, f(Δt), is also derived

$$f(\Delta t) = \frac{1}{N_{tot}} \int_0^T \frac{K^2}{(C+t)^{2p}} e^{-\frac{K\Delta t}{(C+t)^p}} dt \tag{3.5}$$

3.1.3 Waiting time distribution for the Goðabunga catalogue

The waiting time distribution for the Goðabunga catalogue between the years 1993 and 2006 is studied. The catalogue contains over 12000 events of magnitudes ranging between -0.5 to 3.3. The waiting time distribution clearly does not resemble the usually observed Omori aftershock distribution but rather the homogeneous Poisson process where the earthquake rate is approximately constant. With the magnitude of completeness being roughly 1.5 it is clear that most of the events are of similar magnitudes. It is thus perhaps not surprising that the resulting waiting time distribution does not show clear aftershock behaviour.

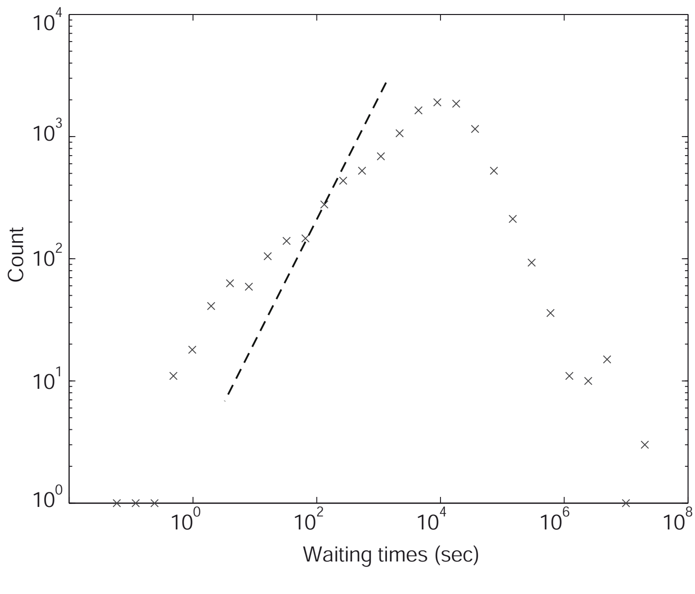

Figure 3.1. The waiting time probability distribution for the Goðabunga catalogue from 1993 to 2006 marked with crosses. The dotted line shows the expected slope of an (infinite) homogeneous Poisson probability distribution.

3.1.4 Seasonal seismicity

Seasonal seismicity has been recognized in various earthquake catalogues e.g. in the Himalaya in Nepal, where winter seismicity is twice as high as the summer seismicity (*Bettinelli et al*., 2007), in Japan, where earthquakes occur rather in spring or during the summer time (*Heki*, 2007), at western United States volcanic centres where peak seismicity occurs at different times for different volcanoes (*Christiansen et al*, 2005) and of course in the Katla/Goðabunga catalogue which will be discussed separately.

In order to explain the modulated seismicity, several models have been presented. *Heki* (2003) noted that in Japan snow covered regions show stronger seasonal variations of seismic activity. Groundwater may play a role in the seismicity in snow regions since meltwater penetrates into cracks of crustal rock and increase the pore pressure there by diffusion.

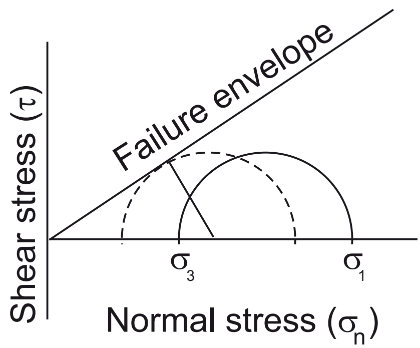

Figure 3.2. The figure shows a Mohr diagram. The straight line is called the failure envelope and represents the strength of the fault (slip on a pre-existing fault). It is assumed that this can be described by $\tau=\tau_0+\mu s_n$, where τ and s_n are the shear and normal stresses resolved on any plane within the material. The parameter μ is termed the coefficient of friction. The solid semi-circle, the Mohr-circle, shows how normal and shear stress vary on planes with different orientation relative to the plane of maximum (s_1) and minimum s_3) principal stresses. Slip is initiated when the Mohr-circle touches the frictional envelope. Increasing pore pressure on faults will lower the effective normal stress and move the Mohr-circle to the left, as indicated by the hatched circle. Here, for the optimally oriented fault the Mohr-circle touches the failure envelope, indicating that the fault will fail. Loading the crust will result in changing the size of the Mohr circle. How the size changes is dependent on the tectonic conditions of the regime in question.

The water flux will induce pore pressure changes. The excess pore pressure reduces the effective normal stress and allows shear stress to move pre-existing faults which are close to failure (*Matsumura* 1986, *Scholz*, 2002). This effect can be demonstrated with a Mohr diagram (Figure 3.2). Although it is highly likely that this phenomenon exists and can explain seasonally modulated seismicity in various places it is non-trivial to evaluate and quantify the effect for snow and ice conditions.

A model of snow load variations as being the cause of seasonal seismicity has also been presented (*Heki*, 2003). The idea is that the snow load enhances normal stress (compression) on the faults and thus reduces the risk of failure by a few kPa. *Heki* (2003) concludes from a case study in Japan that the effect is large enough to modulate the secular stress build-up of a few tens of kPa/yr. Stress changes related to snow load are limited and will not by itself cause slip. It may, however, modulate when during the year slip driven by other factors occurs.

Similarly *Christiansen et al*. (2005) quantify the possible external forcing mechanisms that could modulate seasonal seismicity observed at western United States volcanic centres. They conclude that both snow unloading and groundwater recharge can generate large enough stress changes of >5 kPa at seismogenic depths and may thus contribute to seasonality.

Since the two mechanisms of unloading and increased pore pressure occur close in time and have the same effect of enhancing seismicity, it can be a difficult task to identify the individual processes in the data. Possibly the timing can be slightly different since the unloading has an almost instantaneous elastic response while the penetration of water through the seismogenic crust is a diffusive process which will be reflected as such in the temporal records. With very good seismic records and *a priori* knowledge of the tectonic stresses it might also be possible to evaluate which faults are activated and if their orientation is more consistent with the unloading process or the increased pore pressure.

Recently discovered very low frequency (0.01-0.04 Hz) large magnitude earthquakes (M ~ 4.5-5.2) originating in Greenland outlet glaciers have been shown to be modulated by seasonal changes with more events occurring during the summer months. In addition their number has increased dramatically since 2001, possibly due to warmer climate (*Ekström et al*., 2003).

3.1.5 Seasonal seismicity of the Katla/Goðabunga catalogue

The Katla catalogue, including all the Goðabunga events which truly are the bulk of the catalogue, shows seasonal behaviour. This behaviour was investigated in Paper III and again in Paper IV.

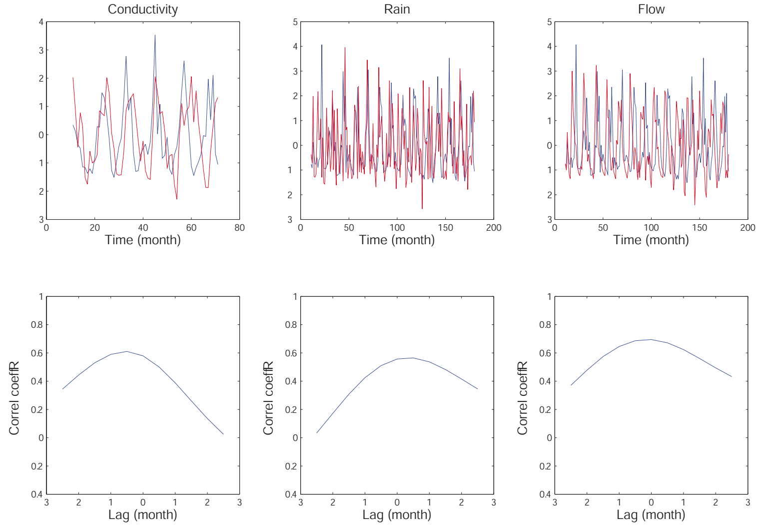

Figure 3.1. Cross correlation analysis between earthquake rate and three other time series. The Goðabunga seismicity catalogue rate (between years 2000-2007) is shown in blue together with conductivity data from Gígjökull glacial lake in northern Eyjafjallajökull, rain data from a weather station south of Mýrdalsjökull and river flow from outlet rivers north of Mýrdalsjökull. Below each time series figure the corresponding correlation coefficient between the two time series is given as a function of time lag.

3.2 Magnitude relations

3.2.1 Gutenberg-Richter relation and the b-value

There are various established methods in seismology which aim at extracting information from large datasets. One of the most established empirical relationships which connects seismic energy and the frequency of seismic events is called the Gutenberg-Richter law (*Gutenberg & Richter*, 1954). It expresses the relationship between the magnitude and the total (cumulative) number of earthquakes in any given region and time period of *at least* that magnitude.

$$\log(N) = a - bM \tag{3.6}$$

Or

$$N = 10^{a-bM} \tag{3.7}$$

N is the number of events with at least the given magnitude M, and a and b are empirical constants.

Using 100 events in a b-value estimation gives according to Aki's maximum likelihood estimate an error of 0.2 (using 95% confidence limits) (Aki, 1965). The relationship is surprisingly robust and does usually not vary significantly from region to region or over time. The constant b is typically equal to 1.0 ± 0.2. This means that for every magnitude 4.0 event there will be approximately 10 magnitude 3.0 earthquakes and 100 magnitude 2.0 earthquakes.

A notable exception is during times of high strain rates such as volcanic earthquake swarms when the b-value can become higher indicating a larger proportion of small earthquakes to large ones. A b-value significantly different from 1.0 may also suggest a problem with the data set; e.g. it is incomplete or contains errors in calculating magnitude. A bend in the Gutenberg-Richter curve is usually observed at low magnitudes corresponding to the magnitude of completeness (Mc) of the data set. This is the magnitude above which our network detects all earthquakes. The a-value indicates the total seismicity rate of the region for the used time period.

Although the relationship is well established and even referred to as a statistical *law*, it is e.g. not clear (when this is written) if it holds for aftershocks occurring very close in time after the main shock and if it holds for very small magnitudes. In addition, even though datasets approximately agree with the Gutenberg-Richter relationship, there maybe some significant deviations which can be of great interest for an improved understanding of earthquake physics. A deviation is commonly observed for large magnitudes where the Gutenberg-Richter straight line seldom fits the data. It should thus be kept in mind that the relationship is empirical.

Båth's law

The other main law describing aftershocks, besides the Omori law, is known as Båth's Law. It states that the difference in magnitude between a main shock and its largest aftershock is approximately constant, independent of the main shock magnitude, typically 1.1-1.2 on the moment magnitude scale.

3.2.2 The magnitude distribution of the Katla catalogue

The magnitude distribution of the Katla catalogue is unusual. It is discussed in Paper III. It is clear from figures 3.4 and 3.5 that the Katla frequeny-magnitude curves are unusual in that they do not show the commonly observed clear log-linear behaviour (constant b-value with slope about one) above the magnitude of completeness.

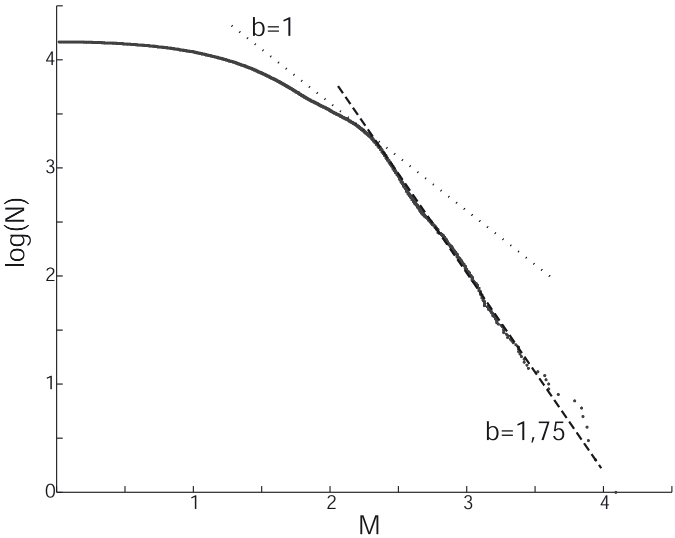

Figure 3.4. The figure shows the Gutenberg-Richter relation for the whole Katla volcano (and Mýrdalsjökull glacier) for the time period between years 1991 and 2006. The normally observed b-value of one does not fit the data. A high b-value of 1.75 fits the data robustly for magnitudes above M2.3

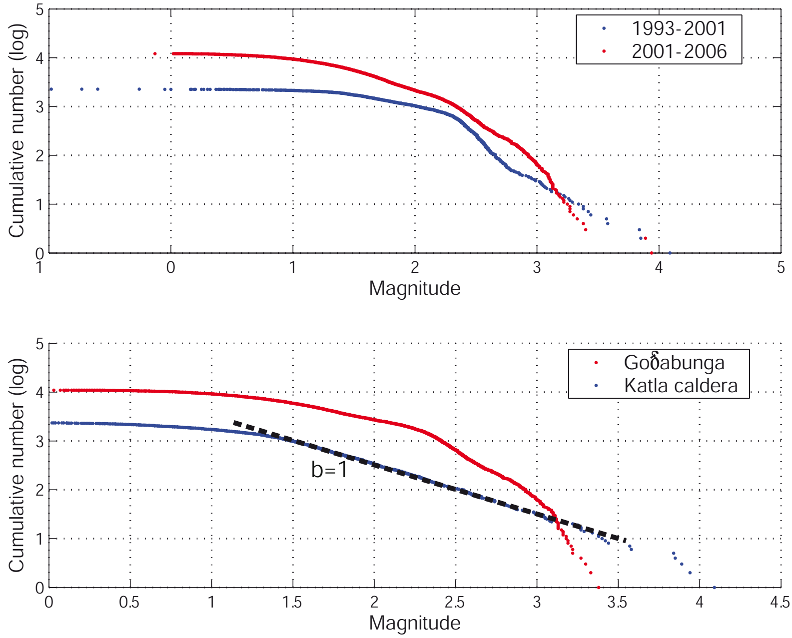

Figure 3.5. Top: In blue we see the Gutenberg-Richter relation for the whole Katla volcano catalogue between years 1993 and 2001. The resulting graph does not fit a single straight line but rather represent at least two populations. In red we see the period between 2001 and 2006 which was dominated by Goðabunga activity. Bottom: A comparison between the Goðabunga and the caldera catalogue reveals that the catalogue from within the caldera behaves as expected, but not the Goðabunga catalogue.

As the SIL network grows and improves, observing capabilities change and so does the magnitude of completeness. Figure 3.6 illustrates the effect of adding a new station (ESK) in the vicinity of the Katla seismicity (the station was moved from a noisy place (south of central Mýrdalsjökull) to the west-north-west, approximately 10 km south of Goðabunga). The b-value curve marked as A represents the year before the station was added to the network (oct 2000-sep 2001) while curve B represents the year after the station was added (oct 2001-sep 2002). The observation capability clearly increases since the magnitude of completeness is lowered from Mc 1.5 down to Mc 1.2 (Mc is marked by arrows on the figure). Using the new Mc value with the data from 2000-2001, we can estimate what the Gutenberg-Richter curve for the seond year would have looked like assuming unchanged seismicity rate, curve C in Figure 3.5. However, increased seismic activity of all magnitudes is observed for 2001-2002, and over 3800 events are recorded instead of the expected 1250 during that year. Therefore curve B is shifted upwards relative to curve C (and A).

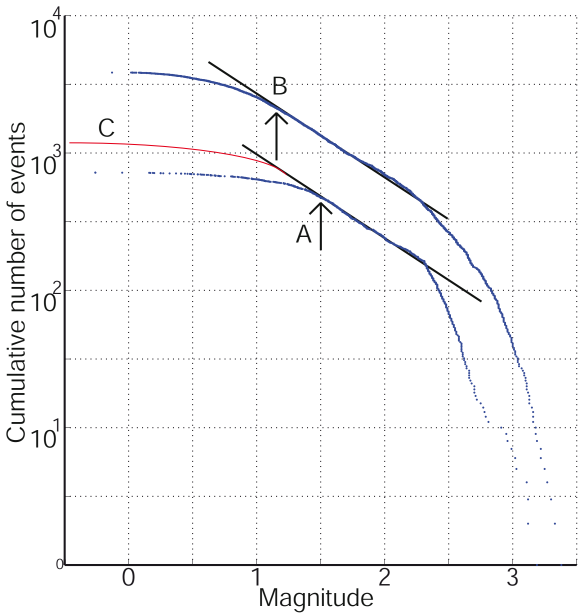

Figure 3.6. The Gutenberg-Richter relation for the Goðabunga catalogue. b-value graph denoted by A, represents the year before station ESK was added south of Katla, (oct 2000-sep 2001). Curve B represents the year after the station was added (oct 2001-sep 2002). The observation capability clearly increases since the magnitude of completeness is lowered from Mc 1.5 down to Mc 1.2 (Mc is marked by arrows on the figure). The curve C represents the expected curve due to the increase observing capabilities of the network the year after the improvement, assuming the same activity level as for curve A.

3.3 Repeated waveforms

Repeating long period (lp) events are often seen in volcanic regions and their repeating nature has been taken as evidence that the source mechanism cannot be destructive, i.e. that the system returns completely to its initial state, supporting models involving fluid flow (*Chouet,* 1996; *Neuberg et al.*, 2000). In Paper IV we present an alternative mechanism to volcanic earthquakes, involving glacial impact events. This mechanism is destructive in the sense that the system has been permanently displaced, but also repetitive. Highly similar waveforms of different earthquakes are due to similar focal mechanisms and common propagation paths and are also observed in non-volcanic environments (see i.e. *Wiens & Snider*, 2001). We thus emphasize that an observation of repeating events in volcanic environments is not by itself an argument for modelling the events in terms of fluid flow.

Repeating events from Goðabunga are illustrated in Figure 3.7.

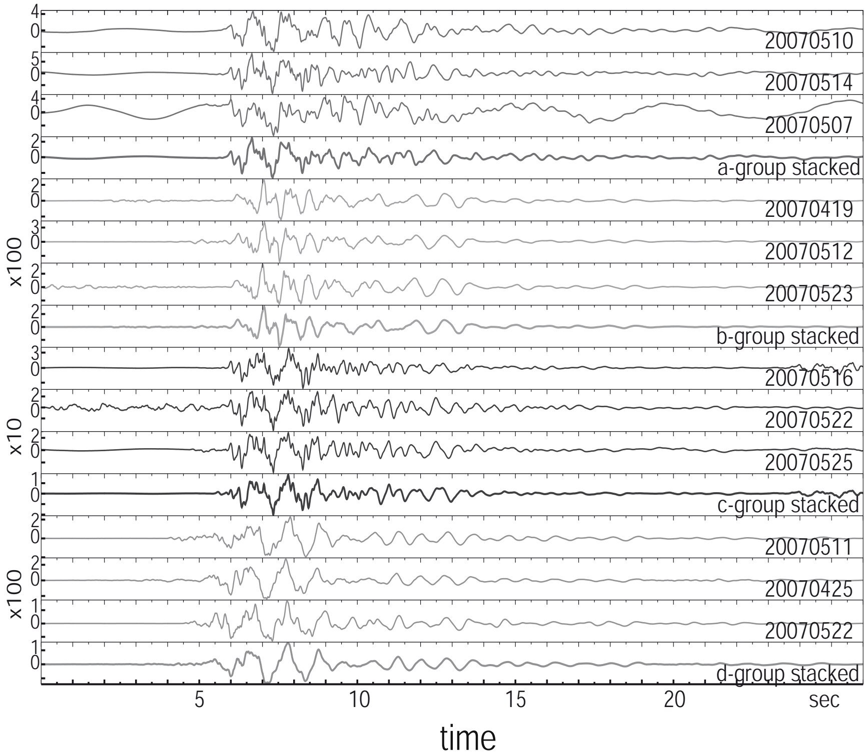

Figure 3.7. Most events recorded in the vicinity of Goðabunga in 2007 can be divided in groups of repeating waveforms. Here we show three events from each group and below a stacked example. Data is unfiltered. Y-axis shows velocity proportional counts (above the eigenfrequency of the instrument, 60 sec).

4 Temporary fieldwork experiment GOD2007

Despite being one of the best covered volcanoes in the country by seismic instruments, the permanent SIL network only estimates the lp events' locations with large errors. It is an extremely difficult task to pick the arrival times of the emergent and unclear phase onsets which additionally look very different even at the closest SIL stations. Further shortcomings of the network include uneven station coverage, with no stations immediately north of the volcano, and the lack of broadband data.

An array analysis, being insensitive of emergent arrivals, can be of great help in order to unravel the complex coda, i.e. it can help us to distinguish between the different phases of the signal and give us information about their slowness and azimuth. The depth of the events needs to be better constrained and it needs to be clarified if the low frequency content of the signal is a path or a source effect. However, such a full suite of seismic analysis requires high quality data from a dense seismic network. This was our motivation to install 10 temporary state-of-the-art broadband seismic stations on Mýrdalsjökull in April 2007, in order to densify the regional (SIL) seismic network.

During the week 16–20 of April in 2007, 10 seismic stations were installed in and around the western flank of the Katla volcano in order to collect data with the aim of elucidating the origin of the persistent and unusual seismicity in the western part of Katla. I will here give a short description of this project seen from the field.

The instruments used were 9 Guralp CMG-3ESP Compact 60 second sensors from Uppsala University and one Lennartz 5 second sensor from the Icelandic Meteorological Office. Guralp (CMG-DM24) digitizers with an attached 40 GB hard disk from Uppsala University were used at all stations. Batteries were borrowed from the Nordic Volcanological Center at the University of Iceland.

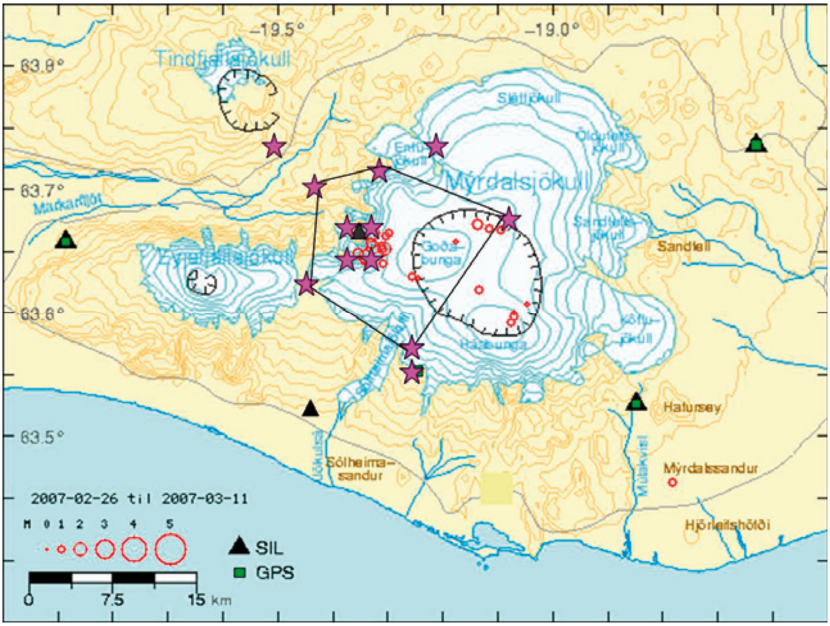

Figure 4.1. The figure shows the station design prior to installation. All possible nunataks in the western part of Mýrdalsjökull are marked with a pink star. Red circles show earthquakes, during a 2 week period, a month before the installation, located with the SIL system which is marked with black triangles. Small green boxes represent GPS stations. (Original figure from SIL web: www.vedur.is)

The experiment was designed in order to meet the following demands in an optimal way:

- Seismic stations should cover the area of the Goðabunga seismicity
- Azimuthal gaps should be minimized
- A seismic array should be installed
- Sensors should be installed on nunataks (places were the bedrock sticks out of the glacier)
- Deployment sites should be reachable by jeeps or snow scooters.

In Figure 4.1 the station design prior to installation is illustrated. We designed our array in such a way that it could reasonably detect a coherent signal at all stations, shifted by a fraction (~0.1-0.3) of its wavelength. Since we were interested in wavelengths of 1-3 km (i.e. body waves with velocity 1,5-3 km/s and with frequencies between 1-3Hz) we estimated that a station spacing of 100-300 m would be optimal.

The realities of the extreme environment forced some deviations from our planning. When we finally got to the field, after waiting for the stormy weather to settle, we realized that some of the nunataks which showed on the maps were not logistically accessible. In addition the station spacing of the array turned out to be much closer to 100 than 300 meters due to space restrictions.

The final station configuration together with the SIL stations is presented in paper IV. A discussion on data retrieval can be found in Paper V.

5 Methods in earthquake seismology

To discuss earthquake seismology in general is clearly beyond the scope of this summary. Since the nature of my thesis is to use many different seismological methods, which for some reason I and my supervisors have found appropriate to use in order to unravel the mysterious Goðabunga seismicity, I will only very briefly summarize the most significant ones.

5.1 The earthquake seismogram

The earthquake seismogram can be treated as the output of a sequence of linear filters, where each filter accounts for some aspect of the seismic source or propagation. It is possible to characterize the elements of a linear filter system by considering the response of the filter to an impulse function. Lets assume that the impulse response of a particular filter f(t) is known and its corresponding Fourier transform is F(ω). Then we can calculate the response y(t) of an arbitrary input, x(t). This is done with the convolution operator and can be done both in the time domain (see equation 5.1) and in the frequency domain (see equation 5.2).

$$F\left(y(t)\right) = F\left(x(t) * f(t)\right) = \int_{-\infty}^{\infty} x(\tau) f(t-\tau) d\tau \tag{5.1}$$

$$F\left(y(t)\right) = F\left(x(t) * f(t)\right) = X(\omega) F(\omega) \tag{5.2}$$

where * represents convolution, X(ω) is the Fourier transform of x(t). (It is far easier to perform a convolution in the frequency domain than in the time domain since in the frequency domain the convolution operator is just multiplication.) If a signal goes through a succession of filters, f_1, f_2, …$f_n(t)$, the output signal is given by the multiple product of the spectra of each filter and the input signal.

The seismogram, u(t) is usually described in terms of three basic filters

$$u(t) = s(t) * g(t) * i(t) \tag{5.3}$$

where s(t) is the signal from the seismic source, g(t) is the propagation filter, sometimes called the Green's function, carrying information about the path from source to the receiver, and i(t) is the instrument response.

In Paper IV we take the advantage of this simple description. By assuming that the lp-events in Goðabunga occur in the same place we argue that a small event, having a very short source time function, can represent the path effect, g(t), i.e. the Green's function. The difference between the seismogram from a big, $u(t)_b$ and a small event, $u(t)_s$ is thus essentially $s(t)_b$ which describes the source time function of the bigger event. We can thus in principle divide their spectra in order to reveal $s(t)_b$. The deconvolution presented in the paper is however performed in the time domain which gave a more stable result.

$$u(t)_b * \left(u(t)_s\right)^{-1} = \int_{-\infty}^{\infty} u(\tau)_b \left(u(t-\tau)_s\right)^{-1} d\tau = s(t) \tag{5.4}$$

5.2 Velocity structure and local earthquake tomography

A common and efficient way of obtaining subsurface information about the velocity structure of a seismically active region is by means of local earthquake tomography. The method, based on P and S wave travel times, is used in Paper III where the Katla volcano is investigated with the aim of identifying structures, such as shallow magma chambers and cryptodomes (postulated by *Guðmundsson et al.*, 1994 and *Soosalu et al.*, 2006, respectively), which might help us unravel the source of the mysterious Goðabunga seismicity. The tomographic inversions presented in this thesis are made using PStomo_eq which allows for simultaneous inversion for both P and S wave velocities as well as hypocentral relocation. (*Tryggvason et al.*, 2002, *Tryggvason & Linde*, 2006).

The simplest case of seismic tomography is to estimate P-wave velocities using P-wave travel times. Since the SIL database also provides S-wave travel times, these are also used in the tomography. Indeed the S-wave velocity and the P and S velocity ratio are very informative when we wish to study volcanic regions. This is because the S-wave is very sensitive to melt inclusions in the rock. Several methods have been developed for this purpose, but here we use 3D local earthquake tomography.

First arrival travel time tomography depends on the general principles of inverse theory discussed in e.g. *Menke* (1989). Generally the aim of the inverse scheme is to invert an observed dataset, here the first-arrival travel times t, to determine a set of model parameters representing some property of the subsurface. Here the model parameter v represents velocity and the hypocentral parameters. Data and model parameters are related by some known function and the forward problem can be formulated as

$$t = \mathrm{L}v \tag{5.5}$$

where L is the forward operator. For a particular set of model parameters the travel times can be predicted using equation 5.5. The tomography inverse problem is thus to find model parameters that minimize the difference between predicted and observed data.

The travel time inversion problem suffers from the fact that the physical properties distribution is a continuous function with very many degrees of freedom, but only a finite number of inaccurate data are measured. As a consequence the inverse problem is non-unique and thus needs to be formulated in a way that includes additional information, regularization constraints and/or prior knowledge about the model. Without constraints, the search for the best fitting velocity model can easily become unstable.

Essential steps in the inversion scheme are

- The forward calculation, compute the first arrival times of seismic waves by solving the wave equation
- Adjust the model parameters (velocity structure and hypocentral locations) to match observed data (travel times).
- Solution assessment.

The forward calculations of travel times are done through a 3D gridded velocity model using a finite difference approximation of the eikonal equation of ray tracing,

$$(\nabla t)^2 = q^2 \tag{5.6}$$

where t is the travel time and q is the slowness (reciprocal of velocity). Travel times are calculated progressively away from the source and by using the travel time field, ray paths can be calculated.

The inversion problem is non-linear. The travel time t of a seismic ray in a continuous velocity medium is given by the line integral

$$t = \int_{l(s(r))} q(r)dl = \int \frac{dl}{v(r)} \tag{5.7}$$

where l is the raypath (between a source and a receiver) which is a function of the slowness q(r) and v(r) is the velocity. Since the integration path depends on the velocity model, the equation is non-linear. The travel time residual relative to the reference model may be caused by a velocity or slowness perturbation anywhere along the path as well as inaccuracies in the source location. The inversion problem is solved iteratively by least squares. Since a change in velocity along the ray will perturb the ray path, new ra paths are calculated iteratively for each model update. The medium is subdivided into blocks of constant properties.

The system of equations for inversion can be described by:

$$\begin{bmatrix} \Delta t \\ 0 \end{bmatrix} = \begin{bmatrix} L \\ k\nabla \end{bmatrix} \Delta q \tag{5.8}$$

were Δt is the travel time residual, L is the raypath matrix from equation (5.5), k is a weight parameter of regularization, ∇ is a smoothness constraint and Δq is the slowness perturbations (measuring the relative perturbation of the current model from the starting model). Regularization is a method to solve mixed-determined problems by applying constraints on the model, in addition to using the data. The goal of the inversion approach is to find a set of model parameters s that minimizes the root mean square misfit of travel times (Δt), given our constraints (regularization and any other constraints which we consider it suitable to apply). We look for models containing "minimum structures", i.e. the simplest models with the least structures necessary to fit the data.

An important step in revealing the velocity structure with tomography methods is building the initial model, since it highly influences the resulting velocity fields after inversion. This step requires some trial and error to find an initial velocity field that results in travel times similar to those observed in the dataset.

The main motivation for model assessment is to determine in what specific ways the solution is non-unique. Different starting models, different free parameters in the model, different constraints, and different subsets of the data are normally tested systematically during assessment of the model and data spaces. In order to estimate the model reliability *Monte Carlo* methods of inverting randomly generated starting models can be used but one of the most common ways of estimating resolution in tomography inversion is to use a checkerboard test. Here the reference model is overprinted by altering patterns of high and low velocity anomalies. Synthetic arrivals are calculated from the altered model and used as input for inversion together with the original source-receiver geometry. The recovered model will show the checkerboard pattern in well resolved regions. In the poorly resolved parts of the model the checks will be smeared or completely absent.

In Paper III we use arrival times from the SIL catalogue, complemented with arrival times from a temporary network of four stations installed on nunataks on Mýrdalsjökull in 2003 to invert the velocity structure. Unfortunately the lack of stations north of the mountain as well as the lack of earthquakes at different depths (the bulk of the dataset is the shallow Goðabunga events) results in a rather coarse velocity model which only reveals the larger structures.

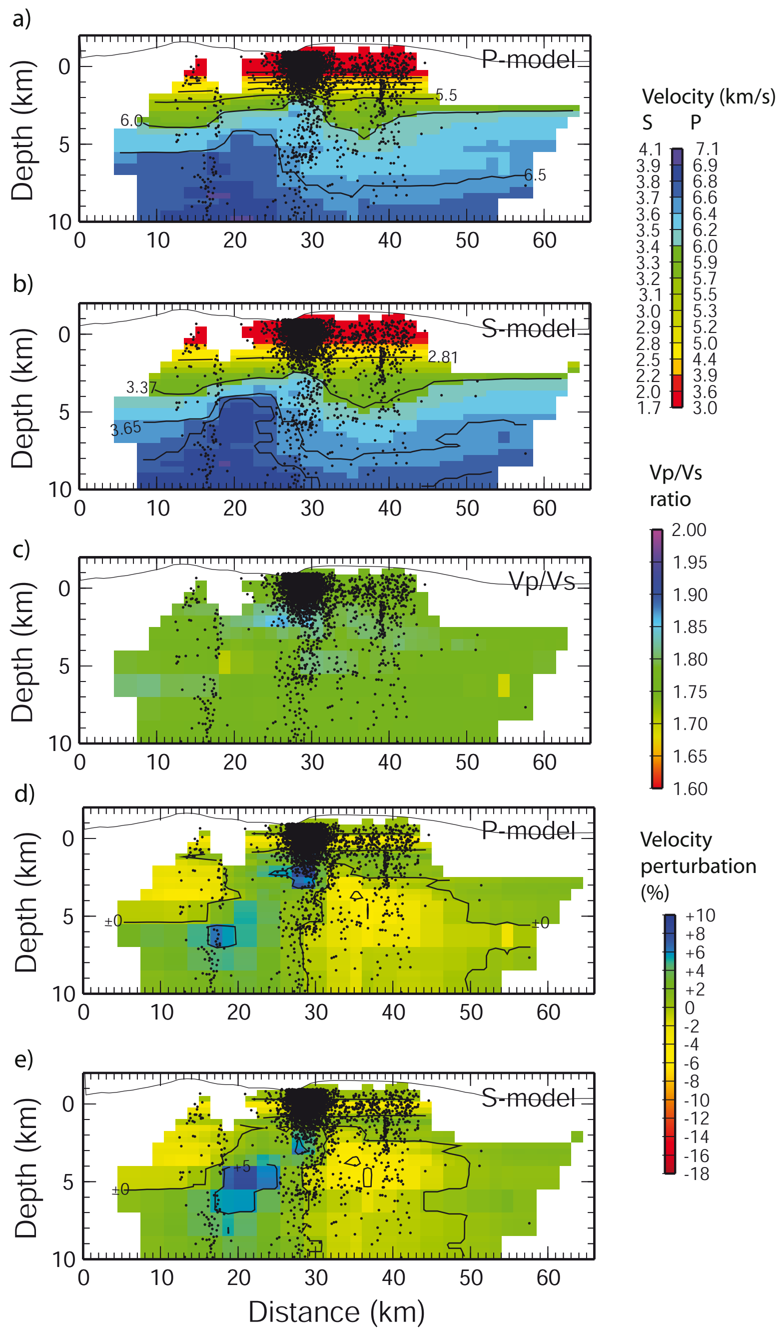

Figure 5.1. Tomographic results from Paper III showing results from an east-west striking profile across the Katla volcano. Cross sections through the final models show also the relocated earthquakes.

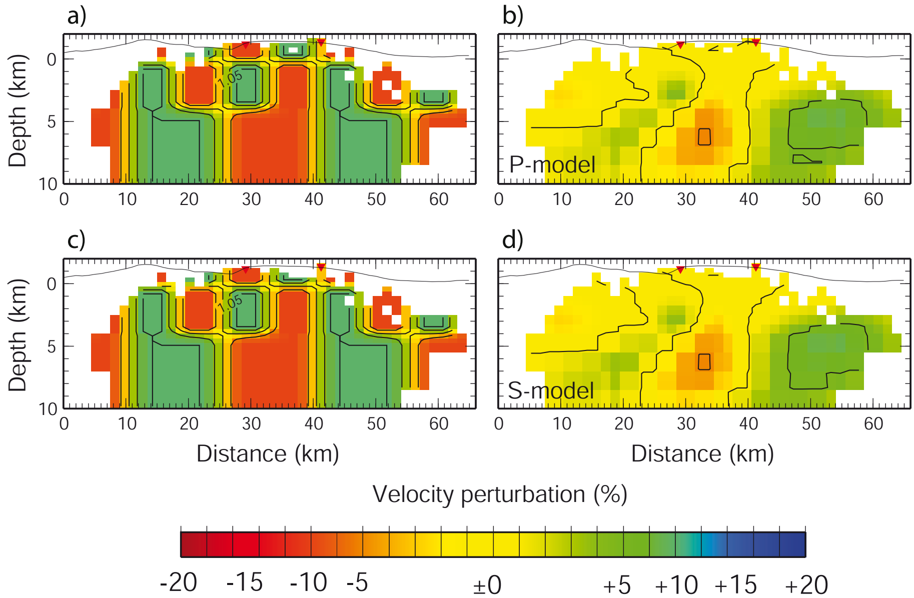

Figure 5.2. Results of resolution tests for the P- and S-wave velocities. The original test model is shown in a) and c) (note they are identical in percentage perturbation) and the results in b) and d) using our models for the P and the S waves respectively.

5.3 Array techniques

Seismic arrays were developed in the 1960's in order to improve detection capabilities for nuclear test monitoring. Their advantage compared to single seismological stations is the improvement of signal-to-noise ratio due to the summation of the individual recordings of the array stations. Seismic arrays can also determine information regarding the direction from which the seismic signals come, and they can be used to locate the source by using a single array measurement

In Paper IV we discuss the results from a mini-array deployment in the vicinity of the Goðabunga events (see discussion on GOD2007). The array was installed in order to improve the locations of the emergent lp-events from the area.

A summary of the most important array techniques, i.e. beam forming and fk-analysis, is given below, following a review paper by *Rost and Thomas* (2002).

5.3.1 Beam forming

Most array methods assume a plane wave arriving at the array. The propagation direction of elastic waves traveling in a laterally homogeneous Earth and arriving at a seismological array can be described by two parameters, the vertical incidence angle *i* and the back azimuth θ (see Figure 5.3). In practice, not the incidence angle i but the inverse of the apparent velocity, v_a of the wave front across the array is used. This parameter is called slowness *u*:

$$u = \frac{1}{v_a} = \frac{\sin(i)}{v_o} \tag{5.9}$$

with v_0 as the medium velocity beneath the array. The back azimuth, θ, is the angle of the wave front arriving at the array measured between north and the direction to the epicenter.

An important use of seismic arrays is the separation of coherent signals and noise. The basic method to separate coherent and incoherent parts of the recorded signal is array beam forming, which uses the differential travel times of the plane wave front due to a specific slowness and back azimuth to individual array stations. If the recordings from individual array stations are appropriately shifted in time, for a certain back azimuth and slowness, all signals with the matching back azimuth and slowness will sum constructively. Appropriate choice of azimuth and slowness should provide the most coherent and thus largest amplitude signal.

Owing to the different locations of the array stations the incident wave front has different travel times to each station. The travel time difference is dependent on the slowness of the wave front and the sensor location. The beam forming method amplifies phases with the appropriate slowness, while suppressing incoherent noise and phases with different slowness. The noise suppression is dependent on the number of stations, N, used for the processing. Given some assumptions, essentially that the signal is identical in each recording and that the noise is completely random and but of the same level at all stations, then the signal-to-noise amplitude ratio should improve by sqrt(N).

The beam forming method works only for a certain slowness and back azimuth combination. Therefore the complete slowness vector of a phase must be known for successful beam forming. Incorrect values of slowness and back azimuth result in lower signal amplitudes and signal distortion. For a successful stack of the waveforms across the array the waveforms must be similar, i.e., coherent. This can complicate the use of beam forming methods for networks with non-uniform station equipment and for large-aperture arrays.

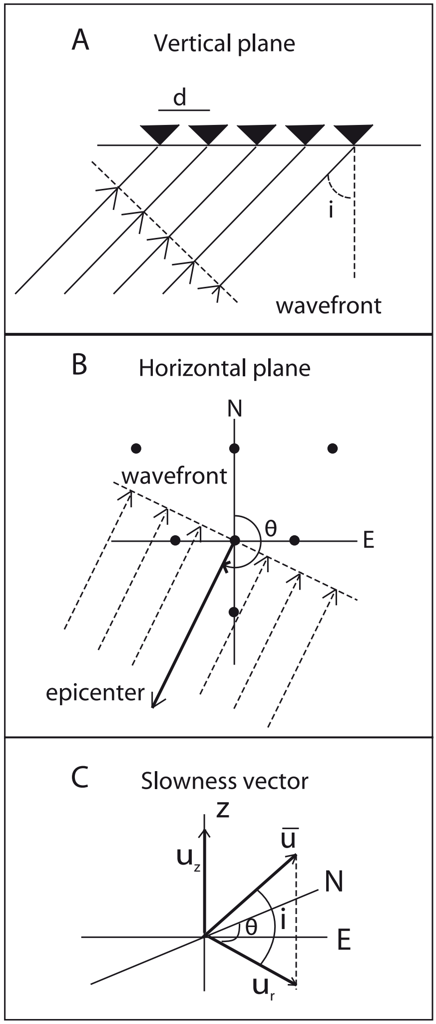

Figure 5.3. a) The vertical plane of an incident (plane) wave front crossing an array (stations marked by black triangles) at an angle of incidence *i*. (b) Sketch of the horizontal plane of an incident plane wave arriving with a back azimuth θ. Stations of the array are marked with filled circles. (Figure has been modified from *Rost and Thomas*, 2002)

5.3.2 Frequency-wave number analysis

Frequency–wave number analysis (fk analysis) is an similar procedure to beam forming, but performed in the spectral domain in essence working with phase-delays at the different frequencies rather than beam forming's time delays (Aki and Richards, 1980).

A seismometer in the array with the location vector r, relative to the array reference point records the signal x (t), with back azimuth θ:

$$x(t) = s(t - \vec{u} \cdot \vec{r}) \tag{5.10}$$

Arrows indicate that the variable is a vector. u is slowness defined as

$$\vec{u} = \frac{1}{v}(\cos\theta, \sin\theta) \tag{5.11}$$

And ν is the medium velocity beneath the array (equation (1)).

The maximum amplitude of the sum of all array seismometers is reached if the signals of all stations are in phase, that is if the time shifts u·r disappear.

The fk analysis can only be applied to short time windows (a few seconds). Large time windows may contain several different phases with different slowness vectors, which make the unambiguous identification of a phase impossible. This implies that the fk analysis is best carried out using arrays for which the delay times of the arriving signal at all stations are small. This disadvantage can be avoided by careful selection of the time windows studied. As with most other array methods, the fk analysis assumes a plane wave front arriving at the array, small heterogeneities beneath the receivers can alter the wave front and destroy the coherency of the signals. This may change the results of the fk analysis.

The total energy E recorded at the array can be defined as the power spectral density, $|S(\omega)|^2$, where $S(\omega)$ is the Fourier transform of the seismic trace, and the array response function, $|A(k - k_0)|^2$, which is controlled by the design (aperture, configuration, and station spacing) of the array.

$$E(k - k_0) = \frac{1}{2\pi} \int_{-\infty}^{\infty} |S(\omega)|^2 \left| A(\vec{k} - \vec{k}_0) \right|^2 d\omega \tag{5.12}$$

Here k is the wave number vector with

$$\vec{k} = (k_x, k_y) = \omega \cdot \vec{u} = \frac{\omega}{v_0}(\cos\theta, \sin\theta) \tag{5.13}$$

and k_0 is the wave number vector for u_0. The back azimuth determines the direction of k and the slowness the magnitude of k.

The result of the fk analysis is power spectral density as a function of slowness and back azimuth. The slowness can be calculated from the wave number vector k = (k_x, k_y):

$$\left|\vec{k}\right| = \sqrt{(k_x^2 + k_y^2)} = \frac{2\pi}{u_r} \tag{5.14}$$

with u_r as the apparent horizontal slowness. The back azimuth θ can be calculated by

$$\theta = \tan^{-1}\left(\frac{k_x}{k_y}\right) \tag{5.15}$$

The power spectral density is displayed in a polar coordinate system called the fk-diagram. In the fk-diagram the back azimuth is plotted on the azimuthal axis, and the slowness is plotted on the radial axis (see Figure 5.4).

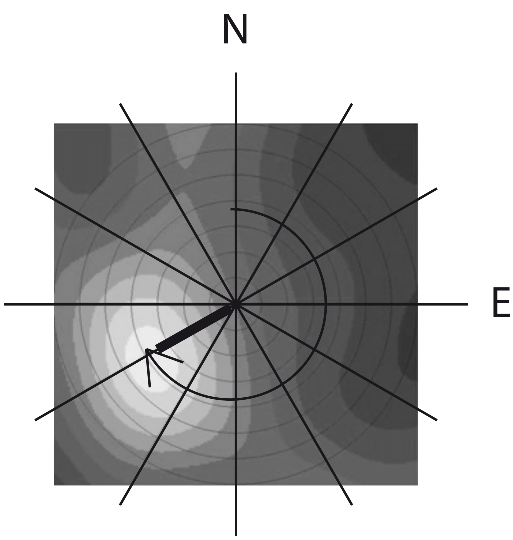

Figure 5.4. FK-diagram showing a pronounced maxima in white where the biggest amplitude of the power spectral density is reached. The analysis reveals a back azimuth of 240 degrees and the slowness can be acquired from the length of the vector (black thick line) from the center of the array to the maxima. (Original figure from the analyzing program Seismic Handler see http://www.seismic-handler.org)

6 Source mechanism of the lp-events registered at Goðabunga

Since the results from Paper IV are so important for my studies I repeat the major findings here below, adding more details of the analysis performed than the journal's length limit allowed. The article is also summarized, along with the other papers, in section 8.

Based on the following observations a hypothesis for the source mechanism of the Goðabunga events is proposed: 1) The seismicity has been continuous for decades and despite the very high deformation rate, manifested in the extreme number of events, there has been no sign of volcanic activity coinciding with the hypocentral locations. 2) Neither InSAR nor GPS measurements reveal any uplift in the area for the last decade that cannot be explained by glacial rebound. 3) The earthquake catalogue for western Katla lacks volcano tectonic events, which can be expected to accompany volcanic intrusion episodes. 4) The seismicity is seasonal pointing to an outside controlling factor. 5) The seismicity rate correlates well with rain and periods of distributed subglacial water channels enhancing glacial motion. 6) The source time function is extended in time. Thus the low frequency content as well as the observed time extended coda can be explained by the source probably to a large extent instead of anomalous path effects. 7) Magnitude distributions show an upper cutoff in magnitude possibly indicating that the deformation field is limited. 8) Repeated waveforms suggest that the source mechanism is repeating and spatially limited. 9) New hypocentral locations coincide with a dramatic ice fall. 10) The far field radiation pattern shows two lobes consistent with a single force source mechanism often used to model surface phenomena such as landslides (*Dahlen*, 1993). 11) Ice fall events have been shown to generate low frequency waveforms (*Roux et al.*, 2008).

We suggest that the lp events occur when ice falls off the escarpment in Tungnakvíslarjökull outlet glacier (see the discussion on Tungnakvíslarjökull in 2.5.1). These events occur throughout the year. However, more events are observed when the ice motion is faster. The rainy season in October induces basal sliding of the outlet glaciers thus speeding up their motion and in our case more ice blocks fall of the cliff.

6.1 Glacier dynamics

In general the hydraulic system inside a glacier consists of a branching system of internal channels that drain the surface of the glaciers via vertical chasms positioned within structural weakness zones of the ice and via porous flow from the firn area into the bed of the glacier (*Benn & Evans*, 1998). At the bed the water either flows in fast lane channels or more slowly in a distributed system of small cavities (*Hooke*, 2005). These two domains seem to coexist within each individual glacier, but the balance between these two operating systems is not constant with time. At periods of more availability of water, channels open at the bed due to more heat transported by the excess water. At times when less water is available the tunnels are suppressed by the ice load and the subglacial water pathways will be dominated by a linked cavity system of drainage (*Kamb*, 1987).

6.1.1 Glacier dynamics at Mýrdalsjökull and Tungnakvíslarjökull

At Mýrdalsjökull glacier the input of melt water from the summer thaw peaks in August (see river flow in Figure 2, Paper IV). Because of the high deformation rate of the steep outlet glaciers in western Mýrdalsjökull, subglacial channels are likely to collapse by ice creep when the melt water discharge starts to diminish. This is normally seen on glaciers as a speed-up in the spring when first melt water reaches the bed and the subglacial channels are not large enough to accommodate the water flux. Water spreads along the bed, decreasing bed friction and increasing basal sliding, which increases the ice flux. This effect is also frequent in the fall, where increasingly colder weather decreases the flux of water into the glacier, and the subglacial channels are compressed by the ice load (*Iken & Truffer*, 1997). Figure 6.1 illustrates the annual changes of the subglacial channels in the form of simple sketches.

In maritime settings, like on Iceland, the cooling in the fall is punctuated by warm and wet periods. During such periods, the plumbing system of the glacier water will not be ready to accommodate water surges, and water will flood the subglacial channels, and likely force fluid into the linked cavity system at the ice - bed interface, decreasing the bed friction and producing ice speed-ups. The area experiences raining in September through November and for the years 2000-2004, heavy rain! This water penetrates through crevasses and is driven into a linked cavity system at the glacier bed (see Figure 6.2). The conductivity measurements confirm this as the conductivity peaks measured downstream indicates water that has been in greater contact with the bed, picking up ions, than water that has mainly been flushed through ice tunnels. At the same time increased water pressure beneath large parts of the steep outlet glaciers likely trigger basal sliding events. Normally basal sliding of glaciers is treated as fairly homogeneous during periods of days – weeks, but as glaciologists study glaciers at higher temporal resolution, they find that the steady flow of a glacier really is a time integral of a plentitude of small scale stress releases (*Pohjola*, 1993).

As the temperature decreases during the winter months and the inflow of water diminishes, the basal water pressure decreases and ice fall events become fewer. Such events have recently been reported as being capable of generating emergent Lp earthquakes of longer duration than normal earthquakes (*Roux et al.*, 2008). Interestingly some properties of these events resemble those reported from volcanoes worldwide which have been related to volcanic activity.

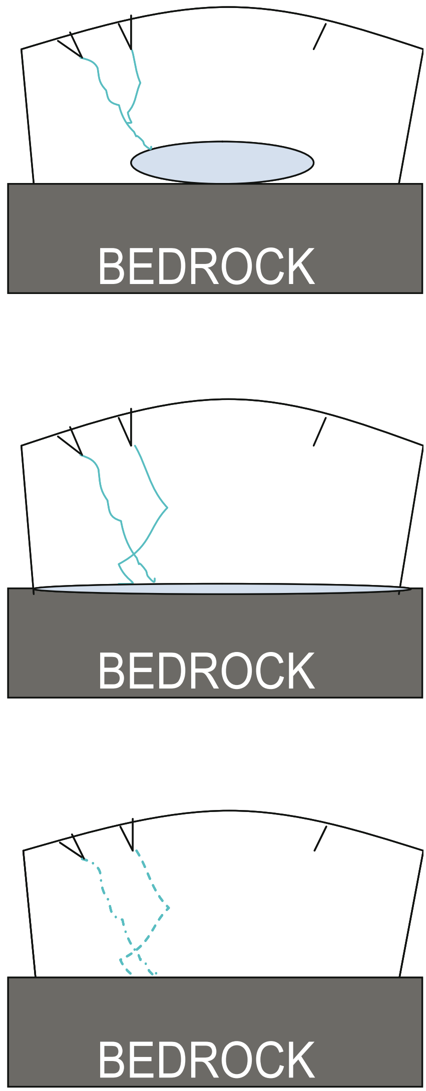

Figure 6.1. From top: Summer (May through August). Water channels are expanding and water runs quickly through the glacier. Low electrical conductivity measured in glacier outlet rivers confirms that. Few lp-events are observed during that period. Middle: Autumn (September through November). Water channels collapse. Heavy rain penetrates through the glacier forming a system of linked cavities. Water runs slowly through the glacier and underlying material and high conductivity is measured. Many lp-events are observed. Bottom: Winter (December through May). No or very little access to water. Few lp-events observed.

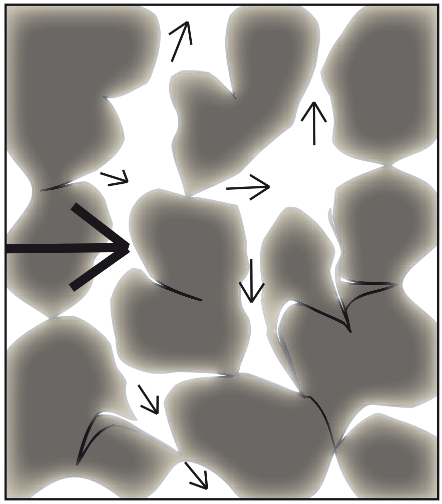

Figure 6.2. Schematic figure of a linked-cavity system at the base of a glacier. Ice motion is described with a thick arrow. Water penetrated through cavities and orifices is in white and its flow is described with the small arrows. (Figure is modifield from Hooke, 2005).

6.2 Ice fall events elsewhere in Iceland?

In Paper IV we associate long-period seismic events with the ice fall in Tungnakvíslarjökull. Is this ice fall unique in Iceland as a producer of lp-events? No, ice fall events do indeed occur elsewhere in Iceland. There are some well known ice-falls in the southern outlet glaciers of Vatnajökull ice cap. Glaciers move and where very steep underlying topography exists the impact of an ice fall can be expected to generate seismic signals – but the size of these will depend on various circumstances. There is every reason to believe that differences in the topography and other factors will mean that the generation of falls effectively creating large seismic events may vary dramatically from place to place.

Another important difference between Mýrdalsjökull glacier and other glaciated areas is the seismic network coverage in Iceland, which does not cover the whole of the island evenly. For example, Vatnajökull glacier is only poorly covered. Therefore we can in principle be missing many ice fall events from these areas.

A preliminary investigation of the SIL catalogue reveals that there exist events with locations in the vicinity of Morsárjökull in southern Vatnajökull. Data from nearby stations to Morsárjökull outlet glacier are presented in

Figure 6.3 and it does in fact appear that similar lp events are registered there. Interestingly the frequencies are mainly between 1-4 Hz similar to the Godabunga events. We also note that the station west of the event (azimuth 90° ± 5°) has particularly strong S-waves which fits a single force model of the ice fall at Morsárjökull.

Clearly, more data and a more thorough analysis is required to confirm that the events are caused by ice fall in Morsárjökull.

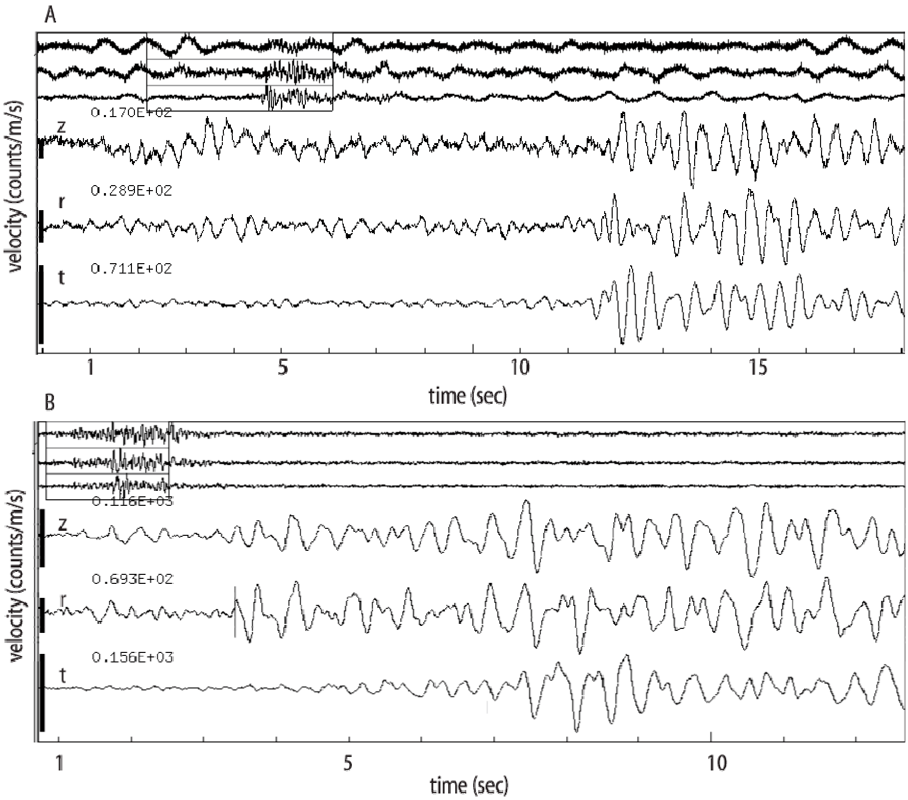

Figure 6.3. Unfiltered velocity seismograms from the two stations closest to the source of a lp-event registered in southern Vatnajökull. In each figure, a zoomed version of the box from the minimized top row showing a longer time series is displayed below. A) Data from Vatnsfell, 82km away from source. Azimuth, estimated from the P-wave polarization is 90° (±5°). B) Closest station, Kálfafell, 23km away from source with azimuth (estimated from P-wave polarization) 50° (±5°). Note that at both the stations we observe similar features to the lp events from Katla, including emergent onset and low frequency content.

7 Very long period near field seismic signals

Recently, there have been several reports of very long period (vlp) signals or pulses, registered on horizontal broadband seismometers, that are only observed in the close vicinity of the source and can thus not be attributed to the normally observed elastic seismic waves. These features are often embedded in earthquake signals of shorter periods. In Paper V we report vlp signals that are embedded in the coda of the largest lp-events recorded with the temporary network in Godabunga in 2007. The signals are analysed in terms of displacement and tilt and compared to models of static displacements that we would expect from the ice fall events. In addition we compared to records from Sweden and discuss possible sources.

Vlp signals are commonly registered in the vicinity of active volcanoes (*Molina et al*., 2008; *Aoyama & Oshima*, 2008; *Wiens et al*., 2005; *Aster et al*, 2003; *Hidayat et al*., 2000; *Wielandt & Forbriger*, 1999). All of these studies suggest that the vlp signals are caused by (static) volumetric changes in the vicinity of the measuring stations. Some interpret them as reflecting elastic wave propagation and apply standard waveform moment tensor inversion methods to elucidate the source characteristics (*Molina et al*., 2008; *Aster et al.,* 2003). A simpler approach considers that the vlp trace is a combination of rotational and translational motions, i.e. tilt and displacement (*Aoyama & Oshima*, 2008; *Hidayat et al*., 2000; *Wielandt & Forbriger*, 1999). The observed linearly polarized vlp signals whose particle motions point consistently to the source are thus often modelled in terms of volcanic expansion phenomena, dyke intrusions and the like.

Parallel to these studies, reports have been made on long-period pulses in broadband records in the near field of earthquakes (*Zahradník & Plesinger*, 2005; *Graizer*, 2006; *Delorey & Vidale*., 2008). The vlp pulses are addressed as artificial signals that need to be removed in order to prevent incorrect analysis of an earthquake's source characteristics. *Delorey & Vidal.* (2008) examine the possibilities that the instrument is producing a non-linear response to an elastic wave or that the instrument is recording a ground motion that is not linear and elastic, as would be the case for permanent deformation. They point out that it is unlikely that non-linear responses of the sensors would manifest themselves on the horizontal output components but not as frequently on the vertical. In addition they note that different instrument types, Streckeisen (STS-2) where the three output components are electronically generated from three identical tilted sensors oriented with azimuths at

120° to each other and Guralp where the three output components are two orthogonal horizontal and one vertical mechanical constructions, show the same behaviour. This observation supports the argument that the cause of the vlp signals is external to the instrument. They conclude that the exact cause of the artefacts currently remains obscure. *Zahradník & Plesinger* (2005) arrive at the same conclusion. They find numerical models of co-seismic permanent displacement (the near field static offset) to be several orders of magnitude lower than what they observe from vlp signals.

7.1 Seismometers and ground motion

A complete understanding of the seismic wave field at a point requires the measurement of 3 components of vector displacement and 3 components of rotation around the perpendicular measuring axes. Seismological practice, using 3 component seismometers, usually assumes that the recorded ground motion represents ground displacement. However, it is well known that horizontal seismometers are particularly sensitive to tilt, which is essentially rotation about a horizontal axis (e.g. *Wieland & Forbriger*, 1999). Very low frequency noise signal registered on the horizontal components has been attributed to tilt caused by diurnal thermal and/or water saturated ground expansion and contraction (*Zuern* et al., 2007).

We use a broad band, 60 second feedback seismometer, CMG-3ESP compact, designed by Guralp Instruments. According to the instrument's specifications, these instruments do not require precise levelling of the sensor package for each component seismometer to work correctly, and static tilts of up to 2.5° are acceptable. In this case, after allowing for the instrument response, each sensor will correctly measure the movement along their axis, but this axis will not be exactly vertical or horizontal. The sensor has a flat velocity response for frequencies above 60 seconds. The sensor has five poles, (-0.074,0.074); (-0.074,-0.074); (-1005.3096,0); (-502.6548,0); (-1130.9734,0)) and two zeros. Generally the transfer function in terms of a Laplace variable s is defined as:

$$H(s) = A\frac{\prod_{n=1}^{N}(s-z_n)}{\prod_{m=1}^{M}(s-p_n)} \tag{7.1}$$

where z_n are the roots of the numerator polynomial and give the zeros of the transfer function, p_m are the roots of the denominator and give the poles of the transfer function and A is a normalising factor designed to make the magnitude of dimension the dimensionless variable H(s) unity over the flat portion of the frequency response (here $A=5.7152*10^8$). It can be convenient to transfer our signal to SI values. In order to do so we need to know the gain constant (in our case G=10000 V/m/s) which is the velocity output sensitivity. In addition we need to know the sensitivity constant (in our case S=3µV/count) of the digitizer. The output signal (in m/s) can thus be described by:

$$Output = \frac{S}{G}(F * H) \tag{7.2}$$

where F is the source function (source time function convolved with the Green's function describing the effects of the source-receiver path).

If a seismometer experiences tilt the gravitational force acts as additional acceleration. When the tilt angle, ɵ, is small this acceleration can be approximated by gɵ, where g is the gravitational acceleration (Aoyama and Oshima 2008).

Wielandt & Forbriger (1999) derive a relationship between the horizontal and vertical output signal produced in the near field of a volumetric source:

$$s_x = C_1 s_z - C_2 \iint s_z \tag{7.3}$$

Here s is the electric output signal or an apparent ground motion in a certain bandwidth. The subscript x represents the radial horizontal signal and z represents the vertical signal. The coefficients C_1 and C_2 have a geometric meaning in that $C_1=X/Z$, where X equals the size of the horizontal radial component and Z the vertical and $C_2=g/L$, where g is the gravitational acceleration and L is the geometrical baseline defined as the ratio between vertical displacement and the tangent of tilt. The waveform of the vertical component is indeed that of the vertical displacement (*Wielandt & Forbriger*, 1999). The equation states that the horizontal signal can be fully deconvolved into two components, i.e. the displacement and tilt.

8 Summary of papers

My thesis contains five papers which I will briefly summarize in the following chapter. The summary involves a description of the main objectives, methodologies, results and conclusions for each paper. A statement of contribution to each study is also given.

Paper I presents the results of modelling simple and fundamental temporal distributions for aftershock sequences and main shocks with the aim of identifying extraordinary temporal distributions in real earthquake data sets from a defined region and time period.

Paper II discusses ‘the unified scaling law for earthquakes’ presented by *Bak et al. (2002) and Christensen et al.* (2002). This is based on waiting time distributions. Using our results of theoretically and numerical simulated earthquake waiting time distributions we conclude that while waiting times are a promising tool for studying large earthquake data sets, their scaling law is seriously flawed.

Paper III summarizes the geophysical observations and structural studies achieved for the Katla volcano at the time the article was written. The paper presents a new study of the velocity structure and of the temporal earthquake behaviour. The source of the lp seismic events is discussed but no conclusions are drawn.

Paper IV concentrates on the lp earthquakes in Goðabunga and their source. The paper presents partly the outcome of the field experiment GOD2007 as well as a more thorough analysis of the seasonal behavior of the Goðabunga seismicity. We conclude that the lp events are caused by glacial deformation, specifically by the impact of ice blocks which fall off an escarpment.

Paper V presents analyses of very long period signals observed with the GOD2007 passive deployment. The signals are only observed in the near field and at the same time as the largest lp events. We discuss physical models that can explain the signals.

8.1 Paper I: Modelling fundamental waiting time distributions for earthquake sequences

8.1.1 Summary

The motivation for this work was to model temporal probability distributions of earthquake sequences in terms of interevent times (waiting times), i.e. the time lag between time-neighbouring events, and investigate the characteristics of these distributions with the aim of distinguishing ordinary temporal distributions from the extraordinary. We derive theoretical equations for the waiting time distribution of an aftershock sequence following the modified Omori law which can be considered to be a fundamental model for the temporal distribution of aftershocks. It is generally described by:

$$\frac{dn}{dt} = \frac{K}{(C+t)^p}$$

Where n is the number of events (aftershocks) following the main shock, K, C and p are empirical constants and t is the time since the main shock (Scholz, 2002). We present numerical simulations of the waiting time distributions of aftershock sequences as well as earthquake sequences following the homogeneous Poisson probability distribution which is often taken as the null hypothesis for main shocks' temporal distribution. We investigate the effect of varying the parameters of the modified Omori law and changing the earthquake rate and the length of the time series. Our results are compared to real data examples of earthquake sequences from four different regions in Iceland.

8.1.2 Conclusions

Our theoretical waiting time distributions agree to first order with the numerical simulations of earthquake sequences following the fundamental models of the modified Omori law and a homogeneous Poisson process which are often take as basic models for aftershock and main shock behaviour respectively. Our models show that the waiting time distribution for a single Omori aftershock sequence consists in general of two power law segments followed by a rapid decay for the largest waiting times. We illustrate our analysis by using real earthquake sequences from four regions: From the Hengill volcanic system during a seismically active period believed to be caused by volcanic intrusion episodes, from two regions around seismic faults in the SISZ which both ruptured in 2000, and from the ice covered Katla volcano. We show that the waiting time distribution from Hengill can be modelled with several aftershock sequences of different rates. The sequences around the two faults that ruptured in the summer of 2000 can be successfully modelled with a single Omori aftershock waiting time distribution.

The waiting time distribution for the Katla volcano catalogue clearly is exceptional and does not seem to contain extensive aftershock sequences and thus follow the Omori law. Instead it shows more resemblance with the homogeneous Poisson distribution. This fact suggests that the Katla catalogue is mainly made up of main shocks and that the underlying process is not diffusive. A possible reason for such a catalogue is that the magnitude of completeness is too high and that the network isn't capable of observing possible smaller events, i.e. aftershocks. We know however that this isn't the case with the Katla catalogue since it spans a range of magnitudes (see Paper III). We conclude that the underlying physical process of the bulk of the Katla earthquake catalogue is not due to normal aftershock processes.

The real data examples investigated suggest that the method of analysing waiting time distribution for specific regions is valuable in order to develop physical models of the underlying processes.

8.1.3 Contribution

K.J. and M.L. carried out the theoretical derivations of the waiting time distributions under the supervision of R.R. K.J. selected data which was analysed cooperatively. The numerical realisations were done by M.L. The paper was largely written by K.J. and R.R. The discussions and conclusions drawn in the paper are a result of a cooperative effort of all the authors.

8.2 Paper II: Earthquakes descaled: On waiting time distributions and scaling laws

8.2.1 Summary

The motivation for this work was to use our knowledge of modelling waiting time distributions in paper I and to investigate and correct several recent papers that present studies of waiting times. Moreover, we present a thorough study of the Unified Scaling Law proposed by *Bak, Christensen, Danon and Scanlon* (*Bak et al.*, 2002, *Christensen et al.*, 2002). They state that all earthquakes follow their new scaling law which combines the Omori law, the Gutenberg Richter law and the fractal dimension for the distribution of earthquake epicentres. The latter two laws enter the new scaling law only in form of two constants used in scaling waiting time distributions in large data sets from a geographical area spanning hundreds of kilometres and spanning tens of years.

Bak et al. (2002) split their data set into many subsets using different magnitude thresholds and spatial cell sizes and present scaled waiting time distributions plotted on top of each other on a log-log graph. In addition they fit the parameters from the three laws experimentally in order to obtain the best possible collapse of the rescaled distributions onto a single curve. The curve obtained has an approximately constant part for the intermediate waiting times and a rapidly decaying part separated by a sharp kink. There is also a segment of decaying waiting times at shorter waiting times. *Bak et al.* (2002) claim that the constant part represents correlated aftershocks, meaning successive earthquakes belonging to the same aftershock sequence while the decaying part represents "uncorrelated" events.

We model waiting time distributions for realistic earthquake datasets resembling those that *Bak et al*. (2002) use in terms of length and rate. We investigate different Omori parameters, the earthquake rate and catalogue length with the aim of explaining features seen in the waiting time distributions, particularly the characteristic kink and the decaying part.

8.2.2 Conclusions

As in Paper I, our numerical and theoretical models of waiting time distributions of aftershock sequences agree and show a power law regime which is followed by a rapid decay for the longest waiting times even for a single Omori aftershock sequence. We illustrate the effect of dividing the catalogue into subsections of different magnitude thresholds on the waiting time distributions (Figure 1 in Paper II).

We model waiting time distributions of Omori sequences of different rates occurring over the same period. Our models show that the location of the bend or kink before the rapid decay for the longest waiting times is dependent on the number of events in the time series. For a large number of events we get fewer longer waiting times and the bend appears at shorter waiting times than when we have a smaller number of events we get longer waiting times and the bend appears later. We investigate the effect of the empirical constant p in the modified Omori Law on the slope of the distributions in the waiting time domain. Our simulations show that the slope generally gives a lower value than p. This is not in agreement with *Bak et al.* (2002) who state that the slope is equal to p.

Our simulations of the same aftershock sequence observed for different lengths of time show clearly that the waiting time distribution for the shortest time series bend downwards at shorter waiting times than the distribution for the longest time series. It is clear that for a single aftershock sequence the "fall off" at long waiting times is purely and completely an artifact due to the limited length of the effective observation period, each aftershock sequence being effectively terminated by the end of the data series or by being drowned by a new aftershock sequence. By numerical simulations we show that the curve obtained by *Bak et al.* (2002) can be modelled by adding Omori sequences of different rates together. We also question *Bak et al.'s* equation for the "fall off" at short waiting times which they claim is simply data loss (inadequate observations at times of high activity rate). This might be regarded as a negative result. However, our modelling shows that the waiting time distributions do contain very useful information in terms of their deviation from an "ideal" double power-law distribution. Using waiting time distributions allows investigation of the properties of large data sets without requiring any (partially subjective) separation into main shocks and aftershocks.

We conclude that the rapid decay at long waiting times is thus a predictable behaviour depending on the length and the rate of the data series used. Furthermore, we conclude that the characteristic kink does not have the physical significance of separating correlated and uncorrelated earthquakes.

8.2.3 Contribution

M.L., K.J. and R.R. jointly analysed "The Unified Scaling Law" presented by *Bak et al*. (2002). The paper was jointly written by the authors. M.L. and K.J. carried out the theoretical derivations of the waiting time distributions in cooperation with R.R. Numerical modelling was carried out by M.L. The discussions and conclusions drawn in the paper are a result of a cooperative effort of all the authors.

8.3 Paper III: Habits of a glacier covered volcano; Seismicity and structure study of the Katla volcano, South Iceland

8.3.1 Summary

Our discovery of the unusual waiting time distribution for the earthquake catalogue of the glacier covered Katla volcano raised a lot of questions regarding the underlying physics. We summarize the studies done so far on Katla, in particular the seismological and other geophysical investigations. The seismological studies indicate that the seismicity can be divided in two areas; seismicity in western Katla often referred to as Goðabunga and seismicity with hypocenters in the glacier covered caldera. Earthquakes belonging to the former group have low frequency seismic signature (*Einarsson & Brandsdóttir*, 2000) whereas the caldera events are more usual high frequency events. We compare the seismicity within these two groups with respect to the magnitude frequency distributions and the temporal distributions as well as comparing the seismic signatures.

The earthquake behaviour is seasonal and this is analysed in detail. The Goðabunga seismicity peaks in October while the less annually correlated caldera seismicity peaks in July/August. Former workers (*Einarsson & Brandsdóttir*, 2000) have suggested that the seasonal earthquake behaviour is a consequence of the combined effects of elevated pore-fluid pressure in the crust and the reduced stress load of the ice cap. We investigate temporal changes of the overburden ice by modelling a snow budget index which is based on climate data together with topographic information on the glacier.

We present for the first time a tomography study of Katla volcano based on data recorded by the permanent SIL network as well as by a temporary network. The data is used to invert for a 3D seismic velocity model underneath Eyjafjallajökull volcano in the west and the Katla volcano in the east. We present a 65 km long and 10 km deep cross-section of the starting velocity models for P and S waves together with the final results. In order to investigate the resolution of our models we present resolution tests for the P- and S-wave velocities where we test velocity perturbations of up to 20% of structures of variable sizes.

8.3.2 Conclusions

We conclude that the Goðabunga seismicity is anomalous in many aspects. The strongly seasonal seismicity points to an outsite controlling factor, most likely hydraulic changes related to the glacier. The different annual behaviour of the caldera seismicity and the Goðabunga seismicity suggest that their sources are fundamentally different.

An estimation of the induced pore-pressure diffusion time suggests that it can be consistent with increased seismicity in July/August and thus explain the induced caldera seismicity. However we find the mechanism unlikely to explain the Goðabunga seismicity. We discuss other hypothesis such as glacial unloading above a pressure sensitive volume, e.g. a magma chamber. We find that the inferred glacial minimum (from snow budget modelling) occurs a month before the Goðabunga seismicity, but such a response should be elastic and thus nearly instantaneous. In addition such a mechanism would be expected to trigger volcano tectonic events.

Velocity images revealed by a 3D local earthquake tomography give a robust picture of the top 10 km beneath Katla. An aseismic high-velocity cone is revealed between Katla and Eyjafjallajökull to the west. A broad structure of low velocity coincides with the structure of the caldera. The fairly constant Vp/Vs ratio in the low-velocity region does not suggest a molten structure of this size. We interpret the structure as a temperature anomaly of a few hundred degrees, in combination with intense fracturing and possibly also hydrothermal circulation. Relocated seismicity generally shows clearer vertical structures but the Goðabunga cluster locates to even shallower depths. The poor station coverage and the lack of deep earthquakes result in a rather low resolution tomography images and structures less than about 7.5 km across cannot be revealed, such as a possible shallow magma chamber beneath the caldera (*Guðmundsson et al.*,1994) or a 1 km wide cryptodome beneath Goðabunga (*Soosalu et al*, 2006).

We conclude that additional earthquake data is desirable for better understanding of the outstanding issues including an analysis of the lp events registered at Goðabunga.

8.3.3 Contribution

K.J. investigated the work done so far on Katla in particular the seismological, geophysical and structural studies. New seismological data was collected in spring 2003 by H.S. where K.J. assisted with the deployment. This data is used together with SIL data in a tomographic study which was carried out by A.T. K.J. prepared the data and together we set up the profile. K.J. carried out the b-value analysis. The seasonal earthquake activity was analysed in close cooperation with R.R., B.L. and R.B. The paper was largely written by K.J., A.T. and R.R. The discussions and conclusions drawn in the paper are a result of a cooperative effort of all the authors.

8.4 Paper IV: Lp-events at Katla volcano, Iceland, are glacial and not volcanic in origin

8.4.1 Summary

The question addressed in this paper is: What is causing the long period earthquake activity in the western part of the Katla volcano? Persistent and seasonally modulated long period earthquake activity has been observed for decades in a glacier covered volcanic environment. The activity has by previous workers been taken as evidence of volcanic unrest. We argue that the nature of the long period events is of glacial origin.

We investigate long period (lp) events registered at Goðabunga from a new temporary deployment of 10 seismic stations, including a mini-array, in the near vicinity of the seismic activity. A study of the source time function suggests that the low frequency extended coda can be attributed to the source. The events can be divided into groups of repeating waveforms suggesting a repeating source mechanism at the same location. An fk-analysis of the array data reveals new locations of the seismicity. Consistently all the events are located in a steep outlet glacier were blocks of 80 km thick ice fall of a 100 m high escarpment.

We present a model of the ice fall events which is consistent in both character and magnitude with seasonal changes in motion of the outlet glaciers based on a joint interpretation of various climatic data together with analysis of the seismic data.

8.4.2 Conclusions

Here we present data together with a model explaining the lp-events observed in the western part of the glacier covered, active volcano Katla. We conclude that the activity is probably not related to volcanic intrusive activity as previously thought, but to ice movements in small but steep outlet glaciers..

The major advance scientific contribution is to show that by a joint interpretation of various climatic data, i.e. electrical conductivity and flow from glacial rivers, precipitation and temperature from nearby weather stations, together with a detailed analysis of seismological data we can come up with a consistent model that explains all our data.

This study discusses volcanic eruptions, earthquakes, glaciers and climate change. A warning of an imminent volcanic eruption has major consequences and it is important that these warnings are as accurate as possible. This study reports on events in the vicinity of a volcano which, like many others, is ice covered. These events were first interpreted as possible eruption precursors, triggering action by the Icelandic National Civil Defence Authority. Our study suggests that the events are in fact not volcanic earthquakes but are caused by harmless movements in the glacier ice. The broad implications are that similar earthquake sequences at other glacier covered volcanoes that are experiencing warmer climate could be expected and identifying them as glacial rather than eruption precursors is vital.

8.4.3 Contribution

R.R., K.J., R.B., B.L., A.T. designed the experiment with the temporary network. K.J. collected and processed data and located events. K.J. spectrally deconvolved earthquakes and calculated synthetic seismograms under the supervision of H.S. A.T. calculated snow budget index. R.R. and K.J. calculated correlation between seismic and climatic data. V.P, K.J., R.R. and B.L. modelled the seasonal changes of the glacier. All authors discussed the results and commented on the manuscript which was largely written by K.J., R.R. and V.P.

8.5 Paper V: Local VLP signals registered at Katla volcano, Iceland

8.5.1 Summary

We report strong and repeating very long period (vlp) signals (10-60 seconds) observed in the data from the temporary installation in spring 2007. The events are observed simultaneously with lp-events of magnitude bigger than M2 resulting in nearly saturated amplitudes at the closest stations. The vlp signals being embedded in the signals from the lp events are revealed with band pass filtering the data. The signals are only observed in the close vicinity of the source and are barely seen at stations 4 km away. They show the largest signal on the radial component but are also observed on the vertical (at the closest stations). Particle motion is close to linear, both in the vertical and horizontal planes. The vertical signals point consistently up, east of the escarpment, and down, west of the escarpment. In the horizontal plane, the particle motion points consistently away from the source, reminiscent of P-wave motion.

We present modeling of static elastic deformation expected to be caused by the ice fall events. We also present and analyze data from Sweden recorded on the same instruments.

Signals showing similar characteristics have recently been reported from the near field of active volcanoes and are generally interpreted in terms of combined tilt and displacement due to volumetric changes of volcanic activity.

Parallel to these studies vlp signals have been reported from the near field of earthquakes. These studies interpret their signals differently than the volcanic studies, not least because the estimated magnitude of tilt is generally much higher than expected from realistic models of static displacement. The most recent papers discuss different alternatives in order to explain the signals but conclude that the explanation for the vlp signals remains obscure.

8.5.2 Conclusions

The observed low frequency signals are not consistent in character with surface waves (everything is clearly in-phase). Given only the data from the near-field stations, the signal might be interpreted as a P-wave from a low frequency source. However, if this were the case, then we would expect the signal also to be clearly observed at more distance stations - and it is not.

Using the vertical signal, the vlp radial signal can be decomposed into (apparent) displacement and tilt components. The estimated tilt component is non-negligible, but not dominant.

The character of the data does not seem be consistent with static displacement due to the sudden shift of a large mass of ice. The relative amplitudes of the vertical and radial displacement components and the estimated tilt are not numerically consistent with such a model and in addition unrealistic mass movements would be needed to explain the observed displacements.

Signals from identical instruments deployed in Sweden have been analyzed in order to try to assess if the signals are instrumental artifacts. One station close to the epicenter of a M4.3 earthquake saturated causing major distortion to the recorded signal, but the character of this signal differs in some ways significantly from the Katla recordings. Another station slightly farther away was near to saturation. Here, low pass filtering reveals a vlp signal. However, this arrives late in the time series, consistent with a surface wave from the source and a clear phase lag is observed between the vertical and radial component, also consistent with a true surface wave. We thus find no indications of some general non-linearity in the instruments which can explain the Katla vlp-data. Since the electric current the instrument can produce in the feedback system is limited, instruments can have problems if a very sharp step in acceleration (tilt) arrives. As far as we have been able to assess, this problem would probably not, however, be able to explain the data we observe.

We discuss some alternative explanations. An unknown generic instrumental effect remains possible, but seems unlikely given the consistent character of the Katla recordings on different (types of) instruments and our investigation of strong signals recorded elsewhere with the same type of instrument. Sound waves are found unlikely to trigger the vlp signals that arrive together with body waves. It is very unlikely that the signals are due to internal instrument failure, as the signals have a clear and consistent character, repeat, and are found in recordings from different instruments. Electromagnetic disturbances are an unlikely cause. It is unlikely to be random tilting behavior since it is repeating in a similar way and shows consistency at different stations. In addition the signals do not appear to be consistent with dynamic tilting caused by a low frequency elastic wave train propagating past the stations.

Possible explanations include some unknown generic deficiency in the instruments, physical tilting and displacement of the instrument caused by a P-wave pushing the instrument in a mostly radial direction, a strain wave of as yet unidentified character, i.e. and unknown static or dynamic deformation effect.

8.5.3 Contribution

K.J. collected and processed data and located events. B.L. modeled the static deformation numerically. All authors analysed the data, discussed the results and commented on the manuscript which was largely written by K.J. and R.R.

9 Summary in Swedish

På Island finns många vulkaner, och flera av dessa är delvis täckta av glaciärer. Vulkanutbrott kan alltid vara farliga, men då dessa istäckta vulkaner får utbrott, kan gigantiska mängder is smältas, med stor flodrisk som följd. En av de större av dessa vulkaner på Island är Katla, som har haft stora utbrott ca 2 gånger per sekel. Enligt sagorna, var Katla en häxa. Hon dräpte en dräng som hade stulit hennes magiska byxor, och gömde kroppen i ett fat med mat. Vartefter att tiden gick, tömdes fatet, och så småningom kom kroppen av stackars Bardi fram. Katla rymde till vulkanen, som numera bär hennes namn, och försvann. Kortdärefter, hade vulkanen utbrott. Forfarande då en utbrott vid Katla tros komma kvoterar islänningarna Katla: “Senn bryddir á Barda” som betyder “Snart kommer Bardi fram”.

Det är länge sedan Katlas senaste utbrott och man har förväntat sig en ny sedan 1960-talet. Än så länge har den onda Katla inte fått utbrott. Hon har dock inte varit helt lugn eftersom många jordskalv har registerats hos Katla. Många av vilka är mycket ovanliga i karaktär. Då antalet jordskalv har ökat i perioder har civilförsvaret på Island blivit oroliga och befarat ett snart utbrott. Detta har dock inte hänt, ännu.

Min avhandling är ett försök att bättre förstå Katla och i synnerhet de ovanliga jordskalven. Bättre kunskap om detta kan leda inte bara till bättre bedömingar av risker från Katla, utan även till djupare förståelse för vulkaner i allmänhet.

På Island, och i andra områden där vulkanutbrott och jordskalv är en del av vardagslivet är det viktigt för invånarna att de aktiva områdena övervakas och granskas med målsättningen att kunna förutsäga kraftiga jordskalv, vulkanutbrott, glaciala översvämningar och andra naturkatastrofer. Därför är det ytterst viktigt att kunna skilja mellan den ”normala” jordskalvsaktiviteten och den onormala. Ett sätt är att analysera hur jordskalv är fördelade i tiden. Jordskalvskataloger domineras oftast av efterskalv som visar diffusivt beteende i tid. Omori-lagen som först upptäcktes på 1800-talet beskriver förloppet bra. För att snabbt kunna analysera stora mängder data är det lämpligt att studera intereventtider, dvs tiden som förflyter mellan två skalv.

Jag har beräknat den statistiska fördelningen för intereventtider för efterskalv som följer Omori lagen och som stämmer överens med numeriska simuleringar. Dessa resultat har ökat vår förståelse av efterskalvsprocessen.

Resultaten visar också att tidigare tolkningar av intereventtider varit felaktiga. Den här sortens studier kan anses vara mycket viktiga eftersom statistiska analyser av stora data mängder är ett verktyg som används för att försöka identifiera de underliggande mönstren i data och därigenom ge insikt i de grundläggande processerna. I de tidigare tolkningar av intereventtidsdata för jordskalv, menade man att intereventtids data gav kraftig stöd för tesen att jordskalv var på en grundläggande nivå egentligen inte förutsebara alls. Om så vore fallet, har det naturligtvis stora konsekvenser för arbetet för att minska jordbävningsrisker, och det är viktigt att vi har kunnat visa att dessa tidigare tolkningar är felaktiga, dvs att intereventtidsdata inte ger stöd till tanken att jordskav är oförutsägbara.

De senaste tjugo åren har man registrerat över hundra tusen jordskalv digitalt från olika aktiva områden på Island. Jag har analyserat delmängder av dessa med avseende på tidsmönster i intereventtiderna. Jag visar att Omorilagen oftast beskriver efterskalvssekvenserna bra, men att det finns viktiga undantag. Ett av dessa undantag är jordskalvsdata från den glaciärtäckta vulkanen Katla på Södra Island som har få efterskalv. Skalven kan delas in i två grupper med avseende på deras lokaliseringar; en som visar vulkanotektoniska skalv inom vulkankratern ner till 15 km djup, och en andra som består av tusentals långperiodiska (lp) grunda jordskalv utan klar första insats i Goðabunga i den västra delen av Katla. Hittintills har man trott att skalven i den senare gruppen orsakas av grunda magmatiska processer, antingen rörelser av magma eller magmatiska gaser in i vulkanen eller samspelet mellan ytprocesser såsom förändringar i grundvatten och snötäcke och den djupare delen av vulkanen.

Lp-skalv registreras ofta vid vulkaner och har visat sig ibland förebåda vulkanutbrott. Lp-skalv i Goðabunga är inte något nytt fenomen utan dessa har registrerats sedan man började göra jordskalvsmätningar i området på 1950-talet. Jordskalven har visat sig ha en årstids- och klimatrelaterad variation. Antalet jordskalv ökar på hösten och är också större under varmare år. Man kan också dela in skalven i grupper baserat på vågformernas karakteristika utseenden, dvs att det finns ett mindre antal av ”karakteristiska” jorskalv som upprepar sig. Man har tidigare tolkat detta som bevis för att jordbävningskällan måste vara ”icke destruktiv”, t.ex. bubblor av magmatiska gaser som då och då tränger sig upp genom magmafyllda ”rör” och producerar de ovanliga markvibrationerna. För att lösa mysteriet med Katlas lp skalv, bedömdes att ny och bättre data behövdes. Därför planerades och genomfördes ett fältkampanj på Katla. Trots det extrema och delvis farliga miljön lyckades vi samla in en ny och unik mängd data som har gett möjlighet att till slut förstå Katla bättre.

En analys av det nya seismiska bredbandsdatat från våren 2007 tyder på att skalven kommer från en glaciärtunga i västra Mýrdalsjökull som täcker Katla. Högt upp i glaciären glider den över en brant klippavsats där stora isflak bryts loss och faller åtminstone 100 m ner på glaciären nedanför. Att signalen har en utdragen källfunktion tyder på att de låga frekvenserna har med källan att göra. Jordskalvens utbredningsmönster och frekvensinnehåll tyder också på att källan snarare liknar jordskred än vanliga jordskalv. Vidare visar sig skalven vara starkt korrelerade med regn. Sammantaget tyder dessa observationer på att signalerna orsakas av isfall. Min nya teori att lp-skalven i området kan relateras till detta fenomen har stor betydelse för övervakningen inte bara vid Katla utan vid många glaciärtäckta vulkaner runt om i världen. Isfall kan naturligtvis vara farliga i närområdet, men inte alls lika farliga som vulkanutbrott. Vårt främsta verktyg för att förutse utbrott är just ökad seismisk aktivitet. Därför om många skalv vid vulkaner runt om i världen som egentligen är isfall istället tolkas som vulkanisk aktivitet kan varningarna brista, särskilt då varmare klimat kan leda till ökade isrörelser.

Det nya seismiska datat visar ett annat fenomen nämligen mycket långperiodiska (vlp) signaler som finns invecklade i vågformen av de större lp-skalven. Dessa signaler finns endast i närområden av källan även om de liknar p-vågor. Liknande fenomen har rapporterats från olika områden i världen, både från vulkaner och från jordskalvsområden. Jämförelse av seismogram från Sverige samt det att signalen i Island mäts på olika slags seismometrar tyder på att vad vi ser är inte något instrumentfel och att signalen är riktig, dvs att den härstammar från utanför instrumenten. Modelleringar av förväntad deformation kring isskalven visar att den observerade signalen verkar inte vara av rätt karaktär och att Katlas isfall är för små för att förklarar datat. Framtida studier kan belysa fenomenet och möjligtvis ge kunskap om ny och hitintills okända processer i närområden av seismiska källor.

Acknowledgments

I would like to begin by thanking my parents who introduced me to Icelandic nature and travelled all around the country with me and my sisters showing us the wonders of the tectonic forces and volcanic features that ornament our beautiful island in the north. I truly thank them for all the support and inspiration they have given me through the years.

I want to acknowledge and thank my supervisor and mentor Roland Roberts. I thank you for your encouragements and persistence. You have opened my eyes to the various methods and ways of thinking in science and particularly in seismology. You have inspired me to grow as a scientist and to develop my skills. You have also been a friend and stood by me in various struggles and been the voice of wise words when needed.

I want to thank my additional supervisors, Reynir Böðvarsson, Björn Lund, Hossein Shomali, Ari Tryggvason, and Ragnar Slunga for guidance and support and for the scientific discussions. In January 2002 I, together with my husband Pálmi, was invited by Reynir to visit Uppsala University and soon after we decided to move with our little son Jón Logi, from Iceland to Sweden. I want to thank Reynir for presenting this opportunity to us and for his friendship through the years. I want to acknowledge Björn Lund for supervising me on various issues and helping me especially to improve my scientific writing. Hossein, thanks for all the patience. I've learned a lot about seismology in practice from you and how to process data in Sac and Matlab. You have been very helpful to me and unselfish with your time. I want to thank Ari for the discussions on structure and tomography, and for the enthusiasm and encouragements. During my first years when Ragnar was here he guided me around the SIL system and explained various things regarding the calculations and the data acquisition and I thank him for that time.

Ari Tryggvason was my first friend in Uppsala. I want to thank you Ari for being there for me especially during my first weeks and months, for showing me around, and introducing me to strange Swedish food (the cinnamon flavoured blood pudding) and customs (mushroom picking, wood chopping and more). I also want to thank Caroline for trying out Afro with me and both of them for all the fabulous dinner parties.

My time here in Uppsala would not have been the same without Björn and Lena and their beautiful children Amanda and Andreas. I want to thank you for all the birthday parties, the dinner parties, the Midsummer fests and so on. I cannot thank you enough for opening up your house and hearts for me and my family.

I want to thank the SNSN team, especially Conny Holmqvist, for the co-operation with the SIL system and the assistance with classifying events.

I also want to acknowledge the SIL team at the Meteorological Office in Iceland, especially Steinunn S. Jakobsdóttir, Kristín Vogfjörð for given me the opportunity to attend Volume meetings, Páll Halldórsson, Halldór Geirsson, Sigurlaug Hjaltadóttir, Jósef Hólmjárn and Matthew Roberts.

I'd like to thank Heidi Soosalu for sharing her data and experience with me and for showing me and my extended family around Tallin.

I want to thank Wallenbergstiftelsen, Liljewalchstiftelsen, Landsvirkjun, Nordvulk, IUGG, INGV, AIV and of course Uppsala University for financially supporting me to attend conferences, summer schools and workshops.

I want to thank Mattias Lindman who worked with me on solving some of the mysteries of waiting time distributions. I learned a lot during that time. Crew power rules! I want to thank my friends that left the department before me; Niklas Linde, Johiris Rodriguez, Lijam Hagos, David Monteroso, Sawasdee Yordkayhun, Paiboon Nuannin, Thomas Kalscheuer, Björn Bergman, Marie Keiding, Sigurlaug Hjaltadóttir and Cedric Schmelzbach. I want to thank Cedric especially for his friendship and being a weekly guest at our house and for joining me and my friends for an unforgettable hike in southern Iceland in all kinds of weather in the summer of 2003. I also want to thank Johiris for the honest attempt to teach us to dance Salsa and for staying in touch since she left. I want to thank Sigurlaug for accompanying me to the strangest concerts in Stockholm and for teaching me that there is more to life than earthquakes (there is also knitting!). Marie, I want to thank you for the time you were here. You are so much fun to be around!

I also want to thank my friends that are around these days. Especially my lovely girl friends Juliane Hübert and Anna Ladenberger -thank you for the music!, Maria De Los Angeles , Eva Karlson, Lena Kashubin, Þóra Árnadóttir and Nina Lebedeva-Ivanova for the saunas and the numerous (lousy..) attempts to exercise at lunch hours and Åsa and Barbara for the girl power theme. The EBC lunch team and especially those who joined the Indian Williams lunch team; Tuna Eken, Sverker Olson, Niklas Juhojuntti, Arnaud Pharasyn. Artem and the Kashubin family I want to thank for their friendship and Russian delights. Niklas Juhojuntti I want to thank especially for really fun parties! I want to thank Chris Hieronymus for the course on Geodynamics, which was inspiring.

I wish to thank my colleagues at Geocentrum. Special thanks to the glaciology team, Veijo and Rickard Petterson, for sharing your experience of glaciers, and to Valentin Troll for sharing volcanic experience. Thanks to the Geophysics professors and staff. I want to thank Siv Petterson especially for helping me out and assisting me with administrative work. I also want to thank Ingegerd Olson for all the help. I want to thank David Gee for the plant and for lively discussions on other more powered plants.

I also want to thank my Icelandic friends, Lovísa & Kiddi, Ásdís & Bjarni, Soffía, Gerða Björk, Ásgeir, Gummi, Helga Lára, Nikkó & Dóra, Gaui, Óli Rögg, Ása, Sigrún, Fríða, Hanna, Rósa, Dedda, Heiða, Linda, Gunnar Hrafn, Vala, Krissa and Dóri. I want to especially thank those who have come to visit me during my time here in Uppsala. Takk Fuglabjarg garg garg!!

I've also made new great Icelandic friends here in Uppsala. Dear Gulla & Össi, Unnar & Árdís, Jóhanna & Gísli, Gunnhildur & Óskar, Heiða & Haffi, Kristín Þórunn, Þóra & Lárus -Thank you for the support and for the friendship!

Last but not least I want to thank my family, especially my sisters Hildur and Gerður and my mother in law Svava.

Finally I want to give my thanks to Pálmi, Álfrún, Jón Logi and Baldur, my never ceasing source of inspiration, support and love.

Errata

In Paper I there are typographical errors in the caption of Figure 6 and two of the equations in Appendix A, equation A1 and A5. In the caption of figure 6 the coordinates of area b) and c) are incorrect. The correct caption for Figure 6 is:

> Fig. 6. A map of the study area in southern Iceland. Triangles show station locations in the SIL network. A) Hengill volcanic area (64.0N-64.15N, 21.0W-21.4W). b) Area around the June 21st (year 2000) main event (M6.5) (63.85N-64.1N, 20.6W-20.9W). c) Area around the June 17th (year 2000) main event (M6.5) (63.85N-64.1N, 20.2W-20.6W). d) Katla volcanic area (Goðabunga) (63.49N-63.8N, 19.25W-19.45W).

In equation A1, the natural logarithm should be used, i.e.:

$$N = K \cdot \left[\ln(C+T) - \ln(C+T_{start})\right] \qquad \text{(A.1)}$$

In equation A5, the stretching of the time between events should take place by raising 10 to the power of **x** (not by multiplying with **x**), i.e.:

$$\bar{t}_{occ} = 10^{\bar{x}} \qquad \text{(A.2)}$$

References

Allen, R. M., G. Nolet, W.J. Morgan, K. Vogfjörð, M. Nettles, G. Ekstrom, B.H. Bergsson, P. Erlendsson, G.R. Foulger, S. Jakobsdóttir, B.R. Julian, M. Pritchard, S. Ragnarsson, R. Stefánsson (2002a), Plume-driven plumbing and crustal formation in Iceland, *J. Geophys. Res., 107 B8, 2163,* doi:10.1029/2001JB000584.

Allen, R. M., G. Nolet, W.J. Morgan, K. Vogfjörð, B.H. Bergsson, P. Erlendsson, G.R. Foulger, S. Jakobsdóttir, B.R. Julian, M. Pritchard, S. Ragnarsson, R. Stefánsson (2002b), Imaging the mantle beneath Iceland using integrated seismological techniques, *J. Geophys. Res., 107 B12, 2325*, doi: 10.1029/2001JB000595.

Aki, K. (1965), Maximum likelihood estimate of b-value in the formula logN=a-bM and its confidence limits, *Bulletin of Earthquake Research Institute, 43, 237-239.*

Aki, K., Richards, P.G., (1980), *Quantitative Seismology, second edition*, Freeman and Co., New York.

Aoyama, H. and H. Oshima (2008), Tilt change recorded by broadband seismometer prior to small phreatic explosion of Meakan-dake volcano, Hokkaido, Japan. *Geophys. Res. Lett. 35*, L06307, doi:10.1029/2007GL032988

Aster, R., S. Mah, P. Kyle, W. McIntosh, N. Dunbar, J. Johnson, M. Ruiz, S. McNamara (2003), Very long period oscillations of Mount Erebus Volcano, *J. Geophys. Res. 108, B11, 2522,* doi:10.1029/2002JB002101.

Árnadóttir, Þ., B. Lund, W. Jiang, and H. Geirsson, H. Björnsson, P. Einarsson, T. Sigurðsson, Glacial rebound and plate spreading: Results from the first countrywide GPS observations in Iceland (in press 2009), *Geophys. J. Int.*, doi: 10.1111/j.1365-246X.2008.04059.x.

Bak, P., K. Christensen, L. Danon and T. Scanlon (2002), Unified Scaling Law for Earthquakes, *Phys. Rev. Lett. 88,* 178501.

Benn, D.I, D.J.A.Evans (1998), *Glaciers and glaciation*, Arnold, London.

Bettinelli, P., J. P. Avouac, M. Flouzat, L. Bollinger, G. Ramillien, S. Rajaure, S. Sapkota (2007), Seasonal variations of seismicity and geodetic strain in the Himalaya induced by surface hydrology, *Earth. Planet. Sci. Lett., 266,* 332-344.

Brandsdóttir B., W. Menke (2008), The seismic structure of Iceland. *Jökull*, 58, 17-34.

Björnsson H., F. Pálsson, M. T. Gudmundsson (2000), Surface and bedrock topography of Mýrdalsjökull, Iceland: the Katla caldera, eruption sites and routes of jökulhlaups. *Jökull, 49,* 29-46.

Bödvarsson, R., S. T. Rögnvaldsson, R. Slunga, E. Kjartansson (1999), The SIL data acquisition systemat present and beyond year 2000, *Phys. Earth Planet Inter., 113*, 89-101.

Christensen, K., L. Danon, T. Scanlon, P. Bak (2002), Unified Scaling Law of Earthquakes, *Natl. Acad. Sci. U.S.A. 99,* 2509-2513.

Christiansen, L. B., S. Hurwitz, M. O. Saar, S. E. Ingebritsen, P. A. Hsieh (2005), Seasonal seismicity at western United States volcanic centers, *Earth Planet.. Sci. Lett., 240,* 307-321. Chouet, B. (1996), Long-period volcano seismicity: Its source and use in eruption forcasting, *Nature, 380, 309-316.*

Chouet, B. (1996), Long-period volcano seismicity: Its source and use in eruption forcasting, *Nature, 380, 309-316.*

Coffin, M. F., L. M. Gahagan, L. A. Lawver (1998), Present-day plate boundary digital data compilation. Technical Report 174, University of Texas Institute for Geophysics.

Darbyshire, F. A., I. T. Bjarnason, R. S. White, Ó. G. Flóvenz (1998), Crustal structure above the Iceland mantle plume imaged by the ICEMELT refraction profile, *Geophys. J. Int. 135,* 1131–1149.

Dahlen, F. A. (1993), Single-force representation of shallow landslide sources*, Bull. Seismol. Soc. Am*., 83, 130-143.

Delorey, A. A., J. Vidale (2008), Broadband Sensor Nonlinearity during Moderate Shaking, *Bull. Seism. Soc. Am., 98(3),* 1595-1601, doi: 10.1785/0120070225.

Einarsson, P. and K. Sæmundsson (1987), Earthquake epicenters 1982-1985 and volcanic systems in Iceland. In: Þ. I. Sigfússon (ed.), *Í hlutarins eðli: Afmælisrit til heiðurs Þorbirni Sigurgeirssyni prófessor,* Menningarsjóður, Reykjavík (in icelandic),

Einarsson, P. (1991), Earthquakes and present-day tectonism in Iceland; Imaging and understanding the lithosphere of Scandinavia and Iceland, *Tectonophysics, 189*, 261-279.

Einarsson, P., B. Brandsdóttir (2000), Earthquakes in the Mýrdalsjökull area, Iceland, 1978-1985: seasonal correlation and connection with volcanoes, *Jökull, 49,* 59-74.

Einarsson, P. (2008), Plate boundaries, rifts and transforms in Iceland. *Jökull, 58*, 35-58.

Ekström, G., M. Nettles, G. A. Abers (2003), Glacial Earthquakes, Science, 24, 302 (5645), 622-624, doi: 10.1126/science.1088057

Graizer, V., (2006), Tilts in strong ground motion, *Bull. Seismol. Soc. Am. 96*, 2090-2102.

Guðmundsson, M.T., Þ. Högnadóttir, A.B. Guðbjörnsson, S. Guðbjörnsson, (2007), Geothermal activity in the subglacial Katla caldera, Iceland, 1999-2005, studied with radar altimetry, *Ann. Glac*., *45*, 66-72.

Gudmundsson, O., B. Brandsdottir, W. Menke, G. E. Sigvaldason 1994: The crustal magma chamber of the Katla volcano in south Iceland revealed by 2-D seismic undershooting. Geophys. J. Int., 119(1), 277-296.

Gutenberg, B., C. Richter, (1954), *Seismicity of the earth and associated phenomena*. Princeton, N.J.: Princeton University Press.

Heki, K. (2003), Snow load and seasonal variation of earthquake occurrence in Japan, *Earth and Plan. Sci. Letters 207*, 159-164, doi:10.1016/S0012-821X(02)01148-2

Hidayat, D., B. Voight, C. Langston, A. Ratdomopurbo, C. Ebeling (2000), Broadband seismic experiment at Merapi Volcano, Java, Indonesia: very-long-period pulses embedded in multiphase earthquakes, *J. Volcanol. Geotherm. Res. Vol. 100,* 215-231.

Holohan E.P., V.R. Troll, T.R. Walter, S. Muenn, S. McDonnell, Z. K. Shipton (2005), Elliptical calderas in active tectonic settings: an experimental approach, *J. Volcanol. Geotherm. Res., Vol. 144,* 119-136.

Hooke, R. LeB. (2005) *Principles of Glacier Mechanics, Second edition*, Cambridge University Press.

Hooper, A., R. Pedersen, (2007), Deformation due to Magma Movement and Ice Unloading at Katla Volcano, Iceland, Detected by Persistent Scatterer InSAR, *Proceedings ENVISAT Symposium*, Montreux.

Iken, A., M. Truffer (1997), The relationship between subglacial water pressure and velocity of Findelengletscher, Switzerland, during its advance and retreat. *J. Glaciol., 43 (144),* 328-338.

Jóhannesson, H., K. Sæmundsson (1998), 1:500000. Tecthonics. Icelandic Institute of Natural History, Reykjavík, 1 edition.

Kagan, Y.Y. (2004), Short-term properties of earthquake catalogs and models of earthquake source, *Bull. Seismol. Soc. Am.*, *94 (4)*, 1207–1228.

Kamb, B. (1987), Glacier surge mechanism based on linked cavity configuration of the basal water conduit system. *J. Geophys. Res., 92,* 9083-9100.

Kanamori, H., J. W. Given, T. Lay (1984), Analysis of seismic body waves excited by the Mount St. Helens eruption of May 18, 1980. *J. Geophys. Res. 89,* 1856-1866.

Lafemina, P.C., T.H. Dixon, R. Maservisi, Þ. Árnadóttir, E. Sturkell, F. Sigmundsson, P. Einarsson (2005), Geodetic GPS measurements in south Iceland: Strain accumulation and partitioning in a propagating ridge system. *J. Geophys. Res. 110, B11405, doi:10.1029/2005JB003675*.

Larsen, G. (2000), Holocene eruptions within the Katla volcanic system, South Iceland: Characteristics and environmental impact. *Jökull 49,* 1-28.

Lindman M., B. Lund, R. Roberts, K. Jónsdóttir (2006), Physics of the Omori law: Inferences from interevent time distributions and pore pressure diffusion modelling. *Tectonophys., 424 (3-4),* 209-222.

Maruyama, T. (1963), On the force equivalents of dynamical elastic dislocations with reference to the earthquake mechanism, *Bull. Earthq. Res. Inst. Univ. Tokyo, 41,* 467-487.

Matsumura, K. (1986), On regional characteristics of seasonal variation of shallow earthquake activities in the world, *Bull. Disas. Prev. Res. Inst. Kyoto Univ. 36,* 43-98.

Menke, W. (1989), Geophysical data analysis: *Discrete inverse theory* (rev. ed.), International Geophysics Series, 45, Academic Press Inc.

Molina, I., H. Kumagai, A. García-Alistizábal, M. Nakano, P. Mothes (2008), Source process of very-long-period events accompanying long-period signals at Cotopaxi Volcano, Ecuador, *J. Volcanol. Geotherm. Res., 176,* 119-133.

Morgan, W.J. (1971), Convection plumes in the lower mantle, *Nature*, 23*0,* 42-43.

Neuberg, J. (2000), Characteristics and causes of shallow seismicity in andesite volcanoes, *Philos. Trans. R. Soc. Lond., A* 358, 1533–1546.

Omori, F. (1894), On aftershocks of earthquakes. *J. Coll. Sci. Imp. Univ. Tokyo, 7,* 111-200.

Óladóttir, B. A., Þ. Þórðarson, G. Larsen, O. Sigmarsson (2007), Survival of the Mýrdalsjökull ice cap through the Holocene thermal maximum: evidence from sulphur contents in Katla tephra layers (Iceland) from the last similar to 8400 years. *Ann. Glaciol., 45,* 183-188.

Pedersen, R., F. Sigmundsson (2004), InSAR based sill model links spatially offset areas of deformation and seismicity for the 1994 unrest episode at Eyjafjallajökull volcano, Iceland, *Geophys. Res. Lett., 31, L14610,* doi:10.1029/2004GL020368.

Pedersen, R., F. Sigmundsson (2006), Temporal development of the 1999 intrusive episode in the Eyjafjallajökull volcano, Iceland, derived from InSAR images, *Bull. Volc., 68,* 377-393.

Peng, Z. G., J. E. Vidale, M. Ishii, A. Helmstetter (2007), Seismicity rate immediately before and after main shock rupture from high-frequency waveforms in Japan. *J. Geophys. Res. 112, B03306,* doi:10.1029/2006JB004386.

Pinel, V., F. Sigmundsson, E. Sturkell, H. Geirsson, P. Einarsson, M. T. Gudmundsson, Þ. Högnadóttir (2007), Discriminating volcano deformation due to magma movements and variable surface loads: application to Katla subglacial volcano, Iceland, *Geophysical J. Int. 169, 325-338,* doi: 10.1111/j.1365-246X.2006.03267.x.

Pohjola, V.A. (1993), TV-video observations of bed and basal sliding on Storglaciären, Sweden, *J. Glaciol., 131,* 111-118.

Rost, S., C. Thomas (2002), Array seismology: methods and applications, *Rev. Geophys. 40, 3, 1008,* doi:10.1029/2000RG000100.

Roux, P. F., D. Marsean, J. P. Metaxian, G. O'Brien, L. Moreau (2008), Microseismic activity within a serac zone in an alpine glacier, *J. Glaciol. 54,* 157-168.

Scharrer, K., O. Spieler, C. Mayer, U. Münzer (2008), Imprints of sub-glacial volcanic activity on a glacier surface-SAR study of Katla volcano, Iceland. *Bull. Volc., 70(4)*, 495-506.

Scholz, C. H. (2002), *The Mechanics of Earthquakes and Faulting*, 2nd edition, Cambridge University Press, Cambridge.

Sigmundsson, F., (2006), *Iceland Geodynamics, Crustal Deformation and. Divergent Plate Tectonics,* Praxis Publishing-Springer Verlag, Chichester, UK.

Sigmundsson, F., P. Einarsson, R. Bilham, E. Sturkell (1995), Rift-transform kinematics in South Iceland: Deformation from Global Positioning System measurements, 1986 to 1992. *J. Geophys. Res.* 100 (B4), 6235-6248.

Soosalu H., K. Jónsdóttir, P. Einarsson (2006), Seismicity crisis at the Katla volcano, Iceland – signs of a cryptodome? *J. Volcanol. Geotherm. Res*., 153, 177-186.

Sturkell, E., Einarsson, P., Roberts, M.J., Geirsson, H., Gudmundsson, M.T., Sigmundsson, F., Pinel, V., Guðmundsson, G.B., Ólafsson, H., & Stefánsson, R. (2008), Seismic and geodetic insights into magma accumulation at Katla subglacial volcano, Iceland: 1999 to 2005, *J Geophys. Res., 113, B03212,* doi:10.1029/2006JB004851.

Sæmundsson, K. (1974), Evolution of the axial rifting zone in northern Iceland and the Tjörnes Fracture Zone, *Geol. Soc. Am. Bull*., 85, 495-504.

Tryggvason, A., S. T. Rögnvaldsson, Ó. G. Flóvenz (2002), Three dimensional imaging of the P- and S-wave velocity structure and earthquake locations beneath southwest Iceland, *Geophys. J. Int., 151,* 848-866.

Tryggvason, A., Linde N. (2006), Local earthquake (LE) tomography with joint inversion for P- and S-wave velocities using structural constraints. *Geophys. Res. Lett., 33, L07303.*

Utsu, T. (1961), A statistical study on the occurrence of aftershocks, *Geophys. Mag., 30: 521-605.*

Utsu, T., Y. Ogata, R. S. Matsuura (1995), The Centenary of the Omori Formula for a Decay Law of Aftershock Activity, *J. Phys. Earth, 43(1):* 1-33.

Vogfjörd, K. S., R. Slunga, M. T. Gudmundsson (2008), Indications of subsurface mass movement in the Katla volcano in Iceland during 1997-2007, revealed by evolution of earthquake locations and geothermal activity within the caldera, as well as crustal deformation around the caldera rim. *Geophys. Res. Abstracts, 10,* EGU2008-A-11308.

Wielandt, E., T. Forbriger (1999), Near-field seismic displacement and tilt associated with the explosive activity of Stromboli, *Ann. Geofis., 42,* 407-416.

Wiens, D. A., N. O. Snider (2001), Repeating Deep Earthquakes: Evidence for Fault Reactivation at Great Depth, *Science, 293,* 1463 - 1466, doi: 10.1126/science.1063042

Wiens, D., S. H. Pozgay, P. J. Shore (2005), Tilt recorded by a portable broadband seismograph: The 2003 eruption of Anatahan Volcano, Mariana Islands, *Geophys. Res. Lett., 32,* L18305*,* doi:10.1029/2005GL023369

Wyss, M., R. Stefánsson (2006), Nucleation points of recent mainshocks in southern Iceland, mapped by b-values. *Bull. Seismol. Soc. Am*., 96(2), 599–608.

Zahradník, J., A. Plesinger (2005), Long-Period Pulses in Broadband Records of Near Earthquakes, *Bull. Seism. Soc. Am., 95(5),* 1928-1939.

Zuern, W., J. Exss, H. Steffen, C. Kroner, T. Jahr, M. Westerhaus, (2007), On reduction of long-period horizontal seismic noise using local barometric pressure. *Geophys. J. Int., 171,* 780-796.

Acta Universitatis Upsaliensis

Digital Comprehensive Summaries of Uppsala Dissertations from the Faculty of Science and Technology 636

Editor: The Dean of the Faculty of Science and Technology

A doctoral dissertation from the Faculty of Science and Technology, Uppsala University, is usually a summary of a number of papers. A few copies of the complete dissertation are kept at major Swedish research libraries, while the summary alone is distributed internationally through the series Digital Comprehensive Summaries of Uppsala Dissertations from the Faculty of Science and Technology. (Prior to January, 2005, the series was published under the title "Comprehensive Summaries of Uppsala Dissertations from the Faculty of Science and Technology".)

Distribution: publications.uu.se
urn:nbn:se:uu:diva-100771

ACTA
UNIVERSITATIS
UPSALIENSIS
UPPSALA
2009